Wear 574–575 (2025) 206093

Contents lists available at ScienceDirect

Wear

journal homepage: www.elsevier.com/locate/wear

Effect of process parameters on the wear characteristics and lapping performance of SLS-fabricated polyamide tools

Dawid Zieliński [a,*], Sisay Workineh Agebo [b], Mariusz Deja [a]

[a] Department of Manufacturing and Production Engineering, Faculty of Mechanical Engineering and Ship Technology, Gdańsk University of Technology, Gabriela Narutowicza Street 11/12, 80 - 233, Gdańsk, Poland

[b] Doctoral School at Gdańsk University of Technology, Gabriela Narutowicza Street 11/12, 80 - 233, Gdańsk, Poland

A R T I C L E I N F O

Keywords:
Rapid tooling
Selective laser sintering
Polyamide
One-sided lapping
Tool wear
Ceramic materials
Technological effects

A B S T R A C T

Nowadays, additive manufacturing (AM) offers new possibilities in the production of tools for various finishing processes, such as grinding, lapping, and polishing. In this study, the effect of different lapping parameters was investigated on the wear characteristics and lapping performance of SLS printed polyamide tools. In accordance with the PS/DK 2^3 experimental design, machining of Al_2O_3 ceramic materials have been conducted on one-sided lapping setup, in which crucial process input factors, such as unit pressure *p*, velocity *v*, and machining time *t*, were considered at upper (+) and lower (−) two different levels. Technological effects related to the material loss of Al_2O_3 ceramic samples, as well as their surface quality based on 2D (Ra, Wa) and 3D (Sa, Sq) roughness and waviness parameters, were analyzed. The experimental results indicated a noticeable influence of the lapping input parameters on the analyzed machining effects, as well as on the shape profile and wear value of the polyamide lapping wheels abrasive segments. Moreover, considering the result of the statistical analysis, mathematical models are developed for the technological effects related to the values of mass material loss Δm, linear material loss Δh, and surface height parameter roughness Ra, in the form of linear regression equations. The developed mathematical models can be used to precisely predict the values of the output variables within the specified range of variation of the parametric settings.

1. Introduction

The basic planarization technique, lapping, is mostly used to obtain parallelism and flatness on the machined surface, and it has become an essential finishing technique in the production of various parts, such as silicon wafers, valve plates, and sealing rings from ceramics [1]. Basically, lapping can be conducted by using a single-sided [2] or double-sided lapping setup [3,4], where a single lapping plate is required for the single-sided lapping technique and two independent lapping plates are needed for the double-sided lapping process. The flatness of lapping plate has a major impact on the machined components' surface quality, dimensions, and form correctness. The intended surface finish, material removal rate (MRR), hardness, surface flatness, and structure of the workpiece all play a significant role in the design and material selection for lapping plate's construction as well as the choice of lapping parameters for machining [5,6]. During machining of semiconductor materials, lapping plates made from cast iron (Fe) and copper (Cu) have been mostly used in abrasive finishing techniques. Due to the economical and easiest fabrication process with the resulting higher material removal rate, lapping plates made of metals are mostly preferable in industrial applications. To obtain a high-quality surface finish, parts are polished after lapping with metallic lapping plates by using a softer tool, such as a plate made of metal-resin composite, tin (Sn), or lead (Pb), through an atomic-level removal of material [7].

Despite significant progress in machining, high requirements imposed by mechanical components make it necessary to develop modern production methods. Additive manufacturing (AM) technologies have been dynamically developing in recent years, showing many advantages associated with the fabrication of elements with complex geometries and structures. Recently, additive manufacturing technologies have become very popular, particularly for abrasive machining applications, such as in the creation of prototype grinding tools, polishing tools, and lapping tools [8,9]. The growing advantage of additive manufacturing technology in the fabrication of end-user parts draws the attention of research in the production of tools for abrasive machining, focusing on the tools feasibility and effectiveness. The use of UV-curable

* Corresponding author.
E-mail address: dawid.zielinski@pg.edu.pl (D. Zieliński).

https://doi.org/10.1016/j.wear.2025.206093
Received 1 February 2025; Received in revised form 9 April 2025; Accepted 22 April 2025
Available online 25 April 2025

Table 1
Recent research investigations in lapping with different conditions.

Type and construction of lapping plates	Process parameters	Abrasive material	Workpiece material	Main machining results	References
Solid cast iron	Unit pressure = 3.79 kPa; Rotational speed of a plate = 64 rev/min; Machining time = 90 min	Mixture of paraffin and oil-based slurry with 98C F500 black silicon carbide grits	Tellurium copper	Δm = 932 mg; Ra = 0.51 μm	(Barylski & Piotrowski, 2019)
Solid cast iron	Lapping speed = 72 rpm; Machining time = 30 min; Slurry = 1 drop/second; Weight of the jig = 0.5 kg	Diamond-suspension liquid containing 20 μm diamond grains	cBN segments	Wear rate decreases as grit toughness increases; Grits with a higher AR wear faster compared to grits with lower AR	(Macerol et al., 2022)
Cast iron lapping platen	Lapping pressure = 13.79 kPa; Speed of lapping platen and the carrier = 40 rev/min; Swing period carrier = 10 s; Machining time = 20 min	50 g lapping paste with diamond abrasive	SiC wafers	MRR = 1768 nm/min; Ra = 97 nm	Jianxiu et al. (2020)
Copper (Cu)-resin lapping plate	Pressure = 4 psi; Head rotation speed = 50 rpm and plate rotation speed = 150 rpm; Flow rate of the diamond slurry = 10 ml/min; Lapping time = 10 min	Diamond slurry at 0.4 wt%	Sapphire substrate	MRR >1.4 μm/min; Ra <0.075 μm	(Pyun et al., 2018)
Segmented resin-bonded plates	Pressure = 1.77 kPa; Plate rotation = 50 rpm; Rim rotation = 5 rpm; Machining time = 60 min	Diamond abrasives embedded in resin	Al_2O_3 ceramics	Ra = 0.182 μm; Δm = 122.43 mg	(Gou et al., 2019)
Segmented SLS-fabricated plates from polyamide PA2200 powder	Unit pressure = 12 kPa; Rotational speed of a plate = 120 rev/min; Speed of guiding ring = 60 rev/min; Machining time = 360 min	Mixture of abrasive paste with SD 28/20 grains and loose D107 diamond grains	Al_2O_3 ceramic materials	Δm = 12.13 g; Sa = 0.83 μm	(Deja, M., Zielinski, D., Agebo, S.W., 2024)

3D printing techniques marked a significant advancement in the production procedures for abrasive tools [10]. UV resin 3D printing technology was used to fabricate a lapping wheel by bonding diamond abrasive particles with resin, and the tool was found essential for machining brittle and difficult-to-cut materials. Compared to iron-based conventional lapping tools, the ultraviolet-curable resin lapping tool was found to improve by 12 % in enhancement of surface roughness and a 25 % lowering of the material removal rate [11]. Additive manufacturing techniques like filament-based fused deposition modeling (FDM) and powder-based selective laser sintering (SLS) found application in the fabrication of tools for grinding [12] and lapping of hard and porous structured ceramic materials [13].

Advanced ceramic materials are become more in demand due to their unique characteristics, such as hardness and porous structure. These materials were categorized under difficult-to-cut materials, and it has been challenging to find effective methods of machining. Due to their resistance to corrosion and owing to high strength, ceramic materials were mostly preferred in the production of mechanical components for aerospace and automotive industries. Additionally, ceramics were used to fabricate cutting tools with different grades for machining heat-resistant superalloys [14]. Ceramic materials made of silicon carbide, zirconia, and alumina have the most potential applications in industries [15]. Aluminum oxide ceramics are known as high-wear-resistance materials, and because of their superior properties at elevated temperatures, they're categorized under difficult-to-cut materials [16]. Oxide ceramics (Al_2O_3) modification by a second phase or reinforcement with TiN particles using laser-assisted methods considerably improved the friction coefficient stability when compared to the alumina monolithic [17]. Conventional machining of ceramic materials made of aluminum oxide resulted in a decreased material removal rate (MRR) and poor surface quality when compared to laser-assisted machining techniques [18]. Machining of ceramic materials is mostly performed using diamond grinding process but due to the brittleness and hardness characteristics of the material, the machined surface is exposed to crack formation and subsurface damage [19,20]. The occurrence of cracking on the surface of machined parts during abrasive machining causes the occurrence of surface flaws, leading the strength and functionality of produced parts to deteriorate. Additionally, due to the friction between the workpiece and grinding tool, high temperature will occur in the machining area, and this leads to the occurrence of burns in the surface, affecting subsurface layers by microstructural transform [21]. Several machining techniques, including single-pass grinding [22], fine grinding [23], chemical mechanical polishing (CMP) [24], and lapping [25], can successfully reduce the subsurface defects, surface waviness, and tool marks that resulted from previous operations.

Due to the kinematics and several technology-based circumstances of the process, lapping is considered a quite complex machining process. The lapping machining station is made up of many components, such as a lapping plate, guiding ring, abrasive slurry or grains, pastes, machining oil, and the samples for machining. These components considerably affect the technological aspects, wear on the lapping tool, and the overall performance of the lapping process. Furthermore, input variables of the lapping process can be categorized as controllable and uncontrollable [1,13]. Lee et al. [26] examined the effect of controllable lapping parameters on self-repairing and processing performance of the lapping wheels using a fixed abrasive platen during single-sided lapping of sapphire substrate. The material removal rate is increased with an increased lapping speed and pressure. Additionally, wear of the tool was delayed because of supplementary addition of lapping slurry. Yin et al. [27] used an ultrasonic-assisted approach for the selection and production of the matching SiC abrasive lapping slurry to explore the impact of abrasive particles on the surface characteristics of sapphire wafers during the lapping process. The abrasive particle size was found to be influencing material removal rate and surface roughness, and the rise in lapping speed and concentration of abrasive grains considerably

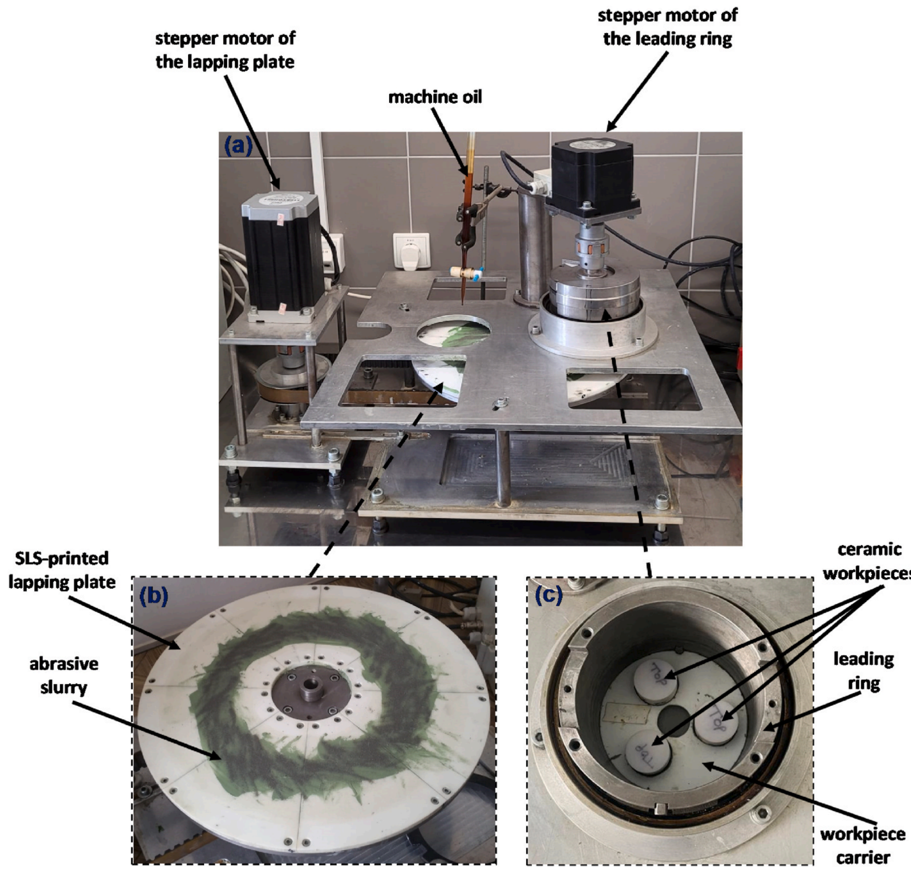

Fig. 1. Experimental setup: a) single sided lapping station, b) detailed view of SLS-printed polyamide lapping plate with abrasive slurry, c) detailed view of Al_2O_3 ceramic samples inside leading ring.

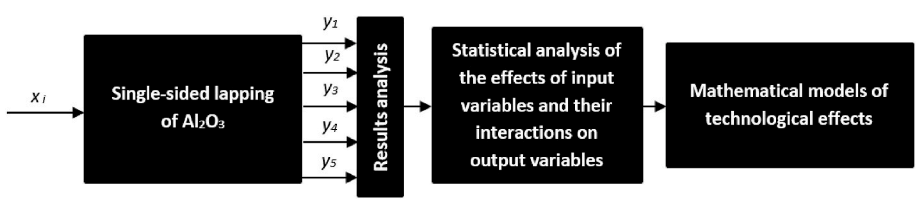

Fig. 2. Scheme of the machining tests of single-sided lapping using different process parameters; characteristics of factors: **X – input variables:** x_1 – unit pressure p: 6; 12 kPa; x_2 – cutting speed v: 0,72; 1,44 m/s; x_3 – lapping time t: 60; 120 min. **Y – output variables:** y_1 – linear material removal *Δh [mm]*, y_2 – surface roughness and waviness parameters: *Ra, Wa [μm]*, y_3 – mass material loss *Δm [g]*, y_4 – 3D surface parameters: *Sa, Sq [μm]* and surface topography *[isometric images]*, y_5 – tool wear *[isometric images, 2D profiles and Wt parameters]*.

improved material removal rate. The study presented in Ref. [28] reports the mixing of two SiC abrasive grits with various sizes and different ratios for free abrasive lapping of wafers, and the performance of the lapping process was significantly improved at high loading mixing of abrasives. A similar study reported that mixing of abrasive grits can improve the material removal process without a significant effect on the surface roughness of silicon wafers under different loading [29]. Xing et al. [30] investigated the effect of ultrasonic-assisted lapping (UAL) for machining diamond/SiC composites considering the material removal mechanism under various machining conditions. The results showed that diamond abrasive sizes found as the most significant influencing factor on the surface morphology at a constant speed of lapping, followed by the ultrasonic average power. The pin-on-disk test was used to investigate the influence of agglomerated diamond abrasive wear on the sapphire machining process, especially on the material removal process. The material removal process mainly occurs due to plastic deformation by the agglomerated diamond abrasive, while the wear of abrasives occur due to attrition and micro-fracture. This affects the diamond grains worn flat and pull out while improving material removal process [31]. An abrasive pad with a uniform pattern of abrasives was fabricated using electroplating and lithography fabrication methods to use for machining sapphire wafers. The study revealed that using a diamond pellet diameter of 12 μm can significantly enhance the surface roughness (Ra) to less than 5 nm [32]. Gao et al. [33] investigated the effect of different-sized abrasives on technological effects during the machining of sapphire substrates with four different vitrified bonded diamond plates. Abrasive sizes of 40 μm and 20 μm resulted in increased material removal with brittle mode, recommending it for rough machining of sapphire substrates. Conversely, grain sizes of 7 μm and 2.5 μm are found in higher and ductile material removal forms while improving the surface roughness (Ra) to 3.5 nm. Experimental comparison of lapping tools performance was evaluated using metal resin platen and fixed diamond abrasive pad while machining sapphire substrates. An improved material removal was obtained with fixed abrasive lapping while deteriorating surface quality when compared to the Cu–resin platen [34].

Table 2
Experimental design matrix based on *PS/DK* 2^3.

Machining test no.	Input variable		
	$x_1 = p$ [kPa]	$x_2 = v$ [m/s]	$x_3 = t$ [min]
1	6 lower level (−)	0.72 lower level (−)	60 lower level (−)
2	12 upper level (+)	0.72 lower level (−)	60 lower level (−)
3	6 lower level (−)	1.44 upper level (+)	60 lower level (−)
4	12 upper level (+)	1.44 upper level (+)	60 lower level (−)
5	6 lower level (−)	0.72 lower level (−)	120 upper level (+)
6	12 upper level (+)	0.72 lower level (−)	120 upper level (+)
7	6 lower level (−)	1.44 upper level (+)	120 upper level (+)
8	12 upper level (+)	1.44 upper level (+)	120 upper level (+)

Much of the studies indicated that lapping is a very complex process involving multiple parameters influencing the performance of the lapping process in terms of machining quality score and tool wear. The quality of the machined output and efficiency of the lapping process are mainly influenced by the lapping parameters and performance of the lapping plate. The literature survey indicates a lack of adequate study in investigating the effects of varying parameters on the wear characteristics of SLS-fabricated polyamide lapping tools. In this study, polyamide lapping plates are fabricated using selective laser-sintering (SLS) 3D printing technique, and the effects of various lapping parameters are evaluated during machining of ceramic materials, Al_2O_3. The influence of machining time, unit pressure, and lapping velocity has been taken into account for the assessment of a 3D-printed polyamide lapping tool's wear and the resulting technological effects, such as material removal and surface roughness. Based on the results obtained, a mathematical model is established to predict lapping responses on the specified ranges of parametric settings. This could provide a comprehensive understanding of the influence of different lapping parameters on the polyamide tools wear characteristics and performance. Overall, the investigations will support the advancing lapping tool fabrication process, especially in additive tool production processes.

2. Overview of related research studies

Lapping, a technique within abrasive machining technologies, has undergone extensive development for many years, yet it is still the topic of many contemporary studies. The technological effects obtained from the lapping process depend on many factors, including unit pressure, kinematic parameters, abrasive suspension characteristics, as well as the type of materials of the lapping tool and workpieces. For this reason, selecting appropriate parameters and process conditions is one of the main challenges for both conventional and newly additively fabricated

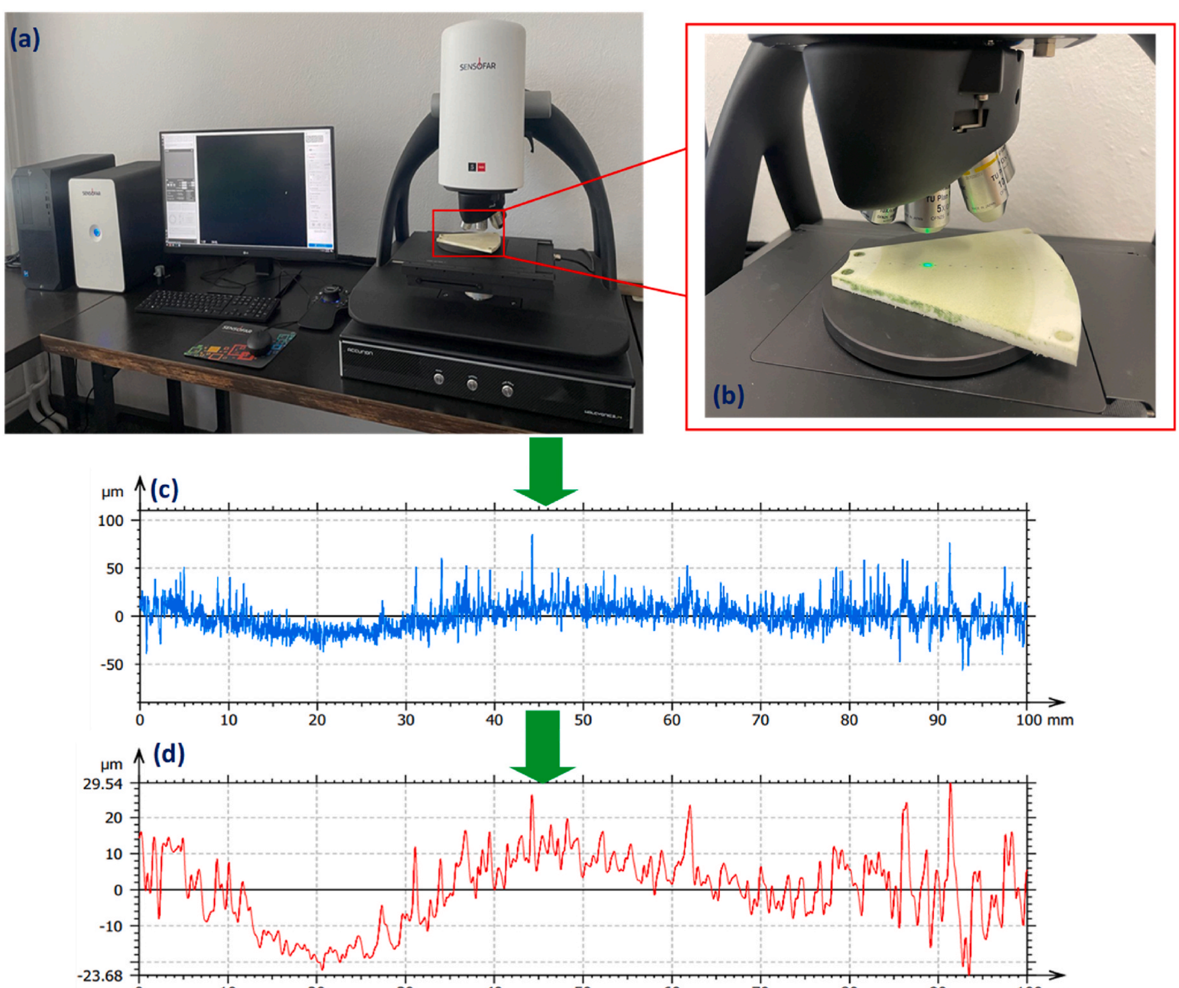

Fig. 3. Measurement station for surface topography assessment: a) Sensofar S neox 3D optical profilometer with lapping segment on the measuring table, b) detailed views of lapping segment during measurement, c) the radial axis raw profile of contact length, d) the radial axis waviness profile of contact length.

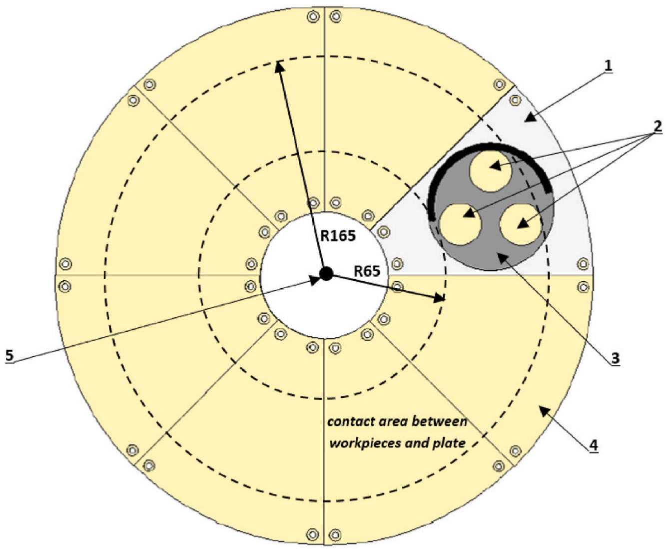

Fig. 4. General kinematic configuration of single-sided lapping station with SLS fabricated abrasive segments; 1 – SLS fabricated single segment, 2 – ceramic workpieces, 3 – workpiece carrier, 4 – lapping plate composed of single segments, 5 – centre of a disc.

tools. Table 1 provides the results of recent research works on the use of different types of tools and lapping conditions.

The influence of kinematic parameters on the solid cast iron lapping tool's active surface uniformity was evaluated using unconventional single-sided lapping, taking into account parameters such as unit pressure and rotational velocity, as well as guiding ring positioning. The positioning of guiding ring had no significant influence on the surface roughness of tellurium copper samples. Whereas material removal rate was improved due to the increment of relative velocity. Additionally, the study revealed that additional movements of the guiding ring result in the occurrence of more even wear on the cast iron lapping tool, and also optimization of the speed ratio can improve the material removal rate and surface roughness of the workpiece [35]. Macerol et al. [36] investigated the wear characteristics of cBN segments by varying the toughness and aspect ratio of grit in the bond system and using solid cast iron plates with 20 μm diameter diamond suspension. The study revealed that abrasive segments with a higher aspect ratio wear faster than lower aspect ratio. The toughness of the grit also plays a major role in the wear behavior of the segments, and it is expected from the experiments that a higher value of grit toughness should decrease the wear rate. However, the higher toughness of the grit resulted in an increased wear rate of the segments. Jianxiu et al. [37] evaluated the effect of various oxidant types and different sizes of abrasive content on the surface roughness and material removal rate of 6H–SiC single-crystal substrate lapping using cast iron platen. Oxidants with their optimum content were observed to having their maximum material removal rate. However, oxidant content and type have an insignificant effect on SiC surface roughness. The combination of improved lapping paste (10 % wt NaOH) and 28 μm in diameter of abrasive particle results in a higher material removal rate of 1768 nm/min and enhanced surface roughness. However, an abrasive size of W3.5 was reported with the lowest surface roughness, Ra 97 nm. Pyun et al. [38] fabricated lapping plates for machining sapphire materials with copper-resin mixes of varying ratios. Aside from the manufacture and assessment of technical impacts, the cu-resin lapping plates are tested with three types of grooves of varying lengths in land, groove, and pitch. The Cu-resin plate with a weight ratio of 50:50 resulted in a better material removal rate and improved surface roughness. However, raising the Cu to 80 % improves material removal, but 100 % results in poor surface roughness and a reduced material removal rate. Plates with grooves performed better while cycling the slurry and increasing the material removal rate. In comparison to pure Cu or resin platens, Cu-resin involved in abrasive particle embedment results in a faster material removal rate and improved sapphire surface quality.

Gou et al. [39] fabricated diamond lapping plates using ultraviolet (UV)-curable additive manufacturing techniques and utilizing resin as a bonding agent. The study evaluated the performance of UV-curable

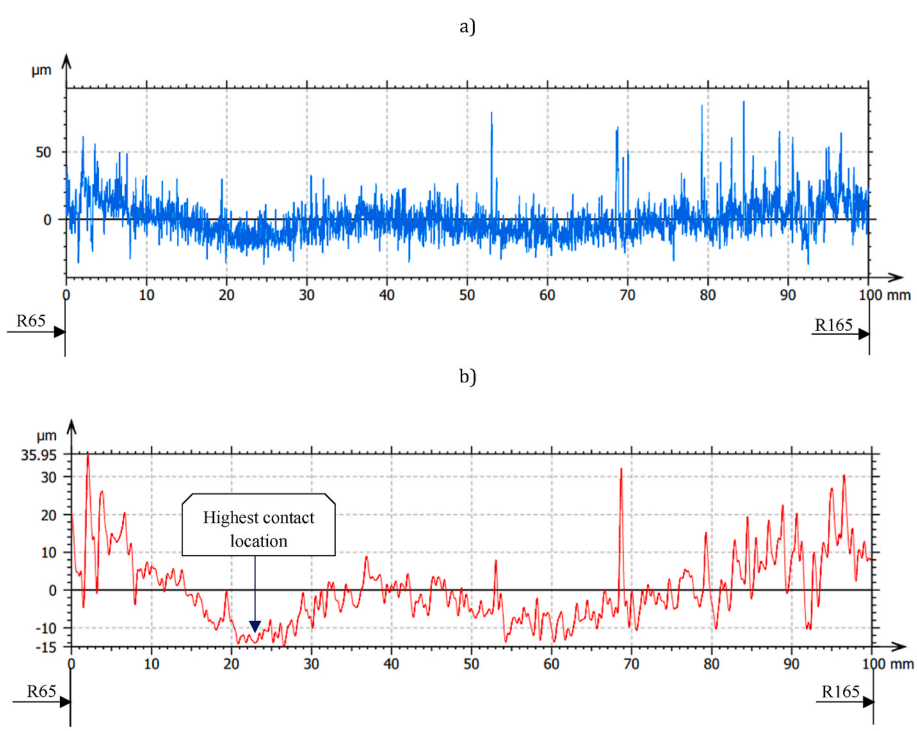

Fig. 5. Exemplary profile of lapping segment #8 after 120 min of machining with p-v- parametric settings: a) raw profile along contact length b) waviness profile along contact length.

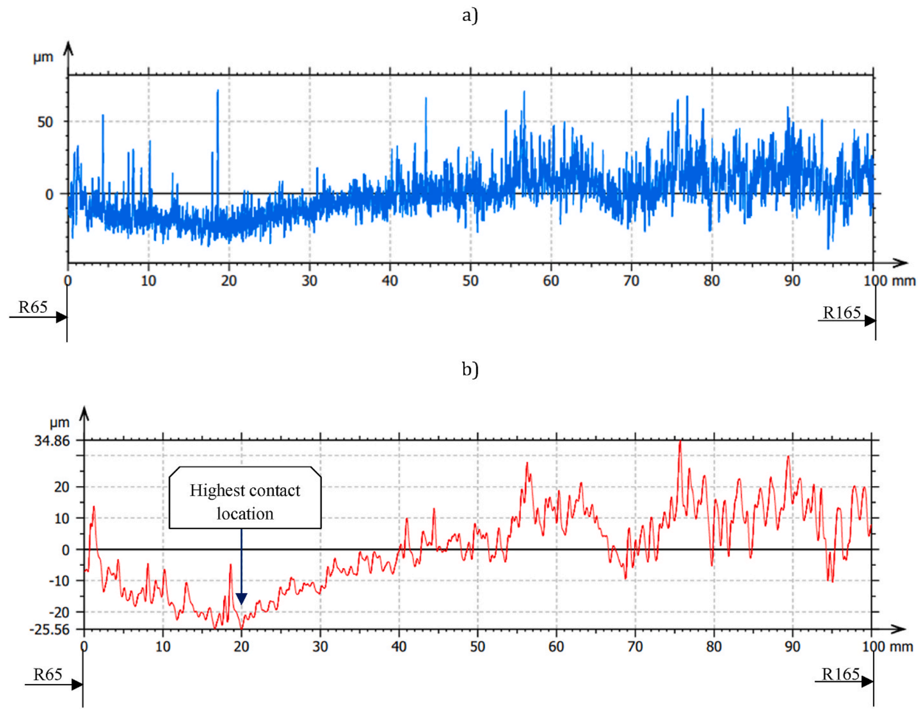

Fig. 6. Exemplary profile of lapping segment #8 after 120 min of machining with p-v+ parametric settings: a) raw profile along contact length b) waviness profile along contact length.

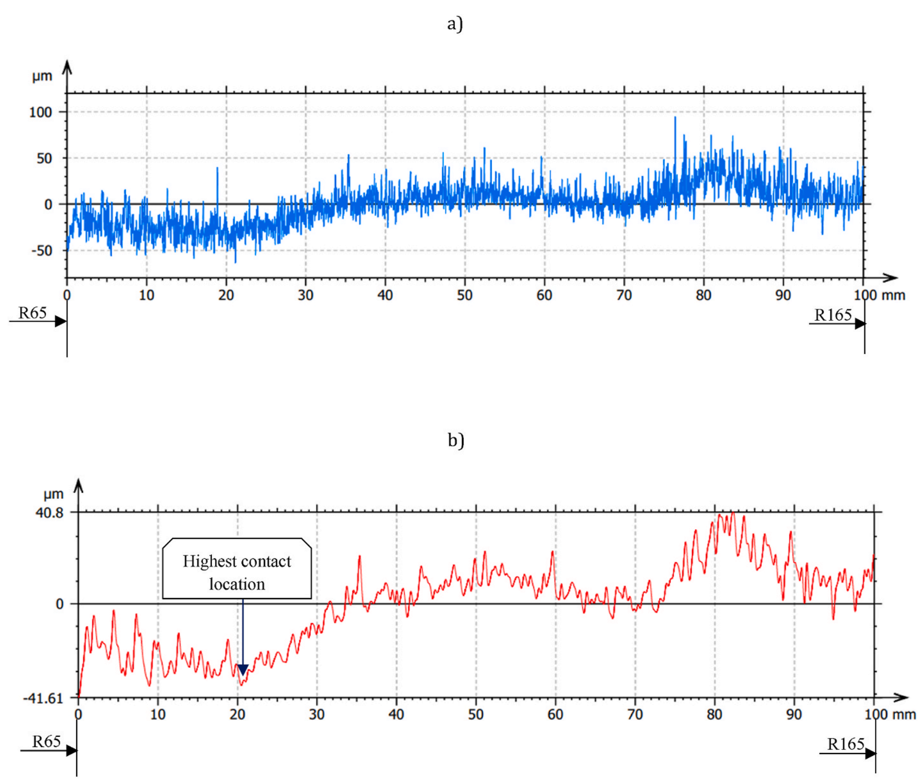

Fig. 7. Exemplary profile of lapping segment #8 after 120 min of machining with p+v-parametric settings: a) raw profile along contact length b) waviness profile along contact length.

diamond lapping plates compared with conventional slurry-based iron lapping plates while machining Al_2O_3 ceramic materials. The ceramic material surface was improved by 12 % with UV-curable resin platen while resulting in a 25 % lower material removal rate comparing to iron lapping plates. The removal of material was initially higher and significantly reduced for UV-curable lapping plates due to fixed abrasive designs of the tool, whereas constant material removal was observed from the iron plate lapping process. In the previous study [40], the wear

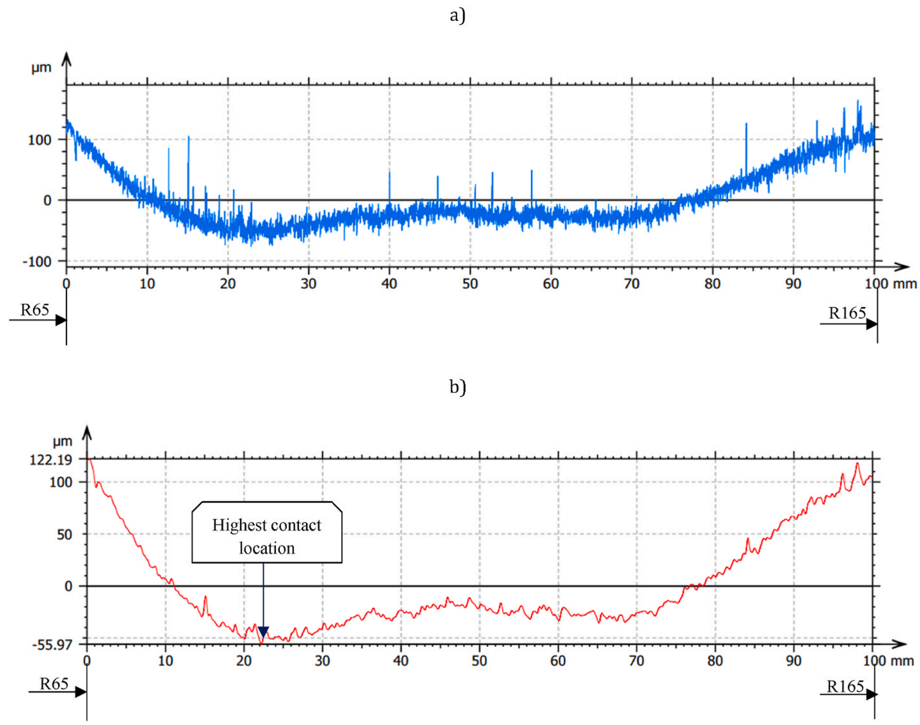

Fig. 8. Exemplary profile of lapping segment #8 after 840 min of machining with p+v+ parametric settings: a) raw profile along contact length b) waviness profile along contact length.

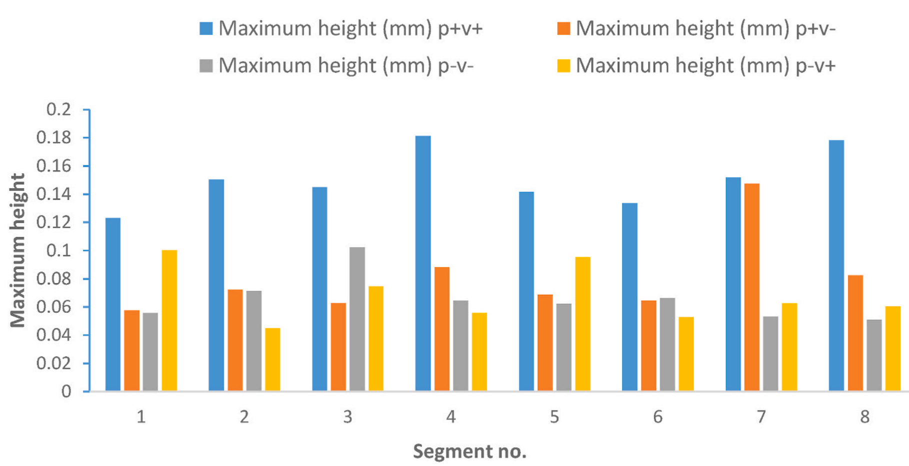

Fig. 9. Parametric maximum height values of the lapping tools segments.

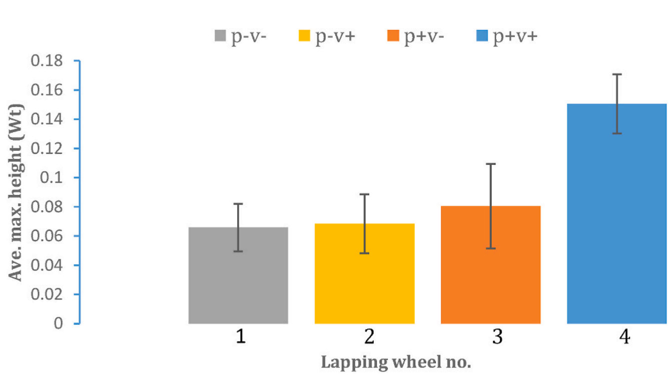

Fig. 10. Average maximum height on the lapping tools wheel.

characteristics of selective laser sintered (SLS) polyamide lapping tool were evaluated for single-sided lapping of technical ceramic material Al_2O_3. The 3D-printed lapping wheel was observed with significant enhancement of the ceramic material surface roughness from the initial value of spatial roughness (Sa) of 1.84 μm–0.83 μm after 120 min of lapping. The abrasive polyamide lapping segment was also observed with the capability of removing material up to 12.13 g within 360 min of machining and 18.43 g of material within 840 min of machining. The study also indicated the highest contact locations on the lapping tool using optical profilometers, and the tool straightness was also analyzed using least squares (LSQ) and minimum zone (MZ) techniques. The results show a non-uniform wear pattern, with the area near the inner radius of the tool with more prominent wear. This SLS-printed tool was found to be an effective abrasive tool for single-sided lapping of Al_2O_3 ceramics, resulting in a lower wear rate, improving surface quality, and providing efficient lapping performance.

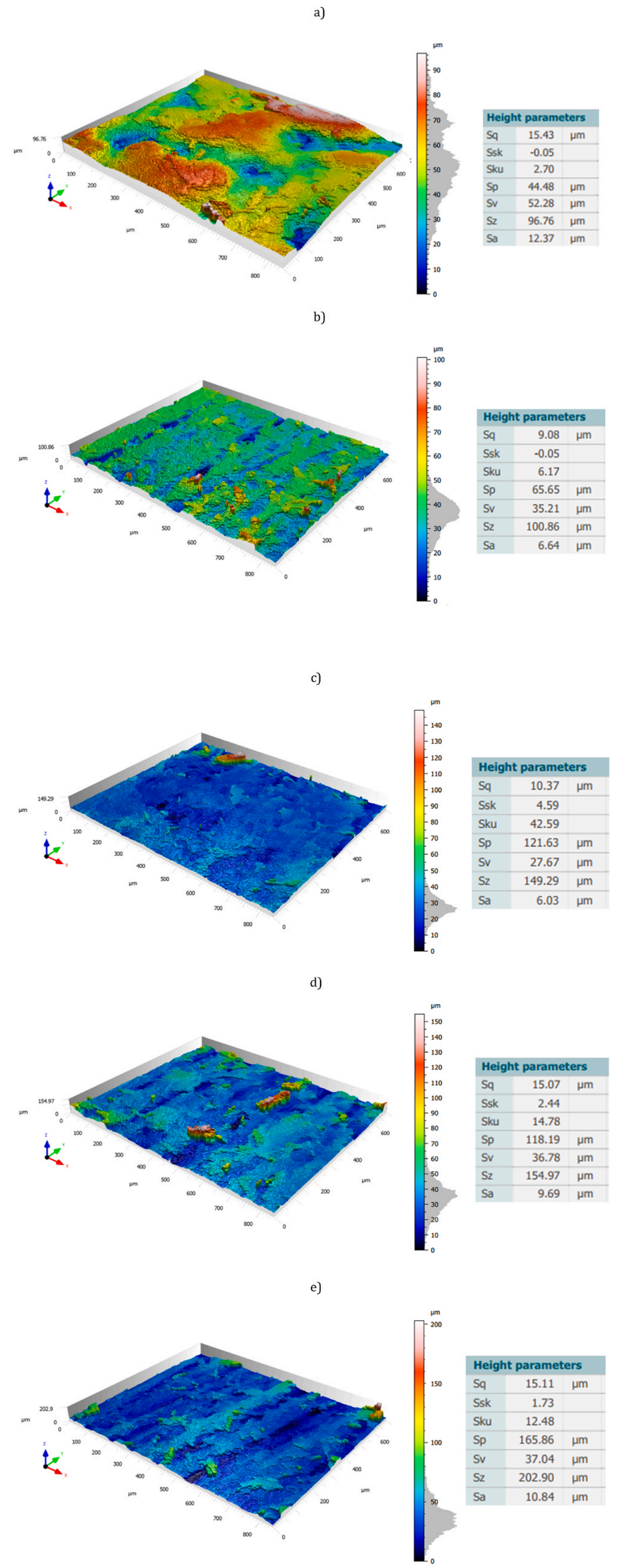

Fig. 11. Exemplary topography of the lapping tools segment #8 on non-contact and highest contact points: a) radius point 55 mm for p-v- b) radius point 85 mm for p-v-, c) radius point 85 mm for p-v+, d) radius point 85 mm for p+v-, e) radius point 85 mm for p+v+.

3. Materials and methods

3.1. Experimental setup and investigation

In this study, SLS-fabricated plates made from polyamide powder PA2200 and a set of Al_2O_3 ceramic samples was used; characteristics have been reported in previous papers [13,40]. Machining tests were conducted on the same one-sided lapping station as shown in Fig. 1, and according to the *PS/DK* 2^3, a two-level static design was determined, and a complete statistical plan was made, where the crucial lapping parameters, such as unit pressure *p*, velocity *v*, and machining time *t*, adopted values at two levels: upper (+) and lower (−) and using *Design of Experiments* module in Statistica software—Fig. 2.

Considering the results of the pilot [13] and systematic [40] studies, the authors decided to perform this study using variable lapping parameters adopting limit values at the upper "+" and lower "-" levels and using equal and constant values for the other factors. The acquired data were utilized to develop mathematical models for selected technological effects associated with the values of mass material loss (Δm), linear material loss (Δh), roughness (Ra), and waviness (Wa), with an assumed significance level of $\alpha = 0.05$. Based on the statistical plan *PS/DK* 2^3 as shown in Table 2, 8 runs of machining tests were carried out, each time using a new lapping plate printed by the SLS method and a new set of three samples from Al_2O_3. Similar to previous studies, it is decided to use the same type of abrasive slurry containing 4 ml of *SD1/0* abrasive paste and 2.5 ml of *D107* loose diamond grains, which was also applied only once to the surface of the wheel before the start of a given experiment test, as well as a dosing of machine oil at a flow rate of ≈0.1 ml/min.

3.2. Measurement methods

Linear and mass material losses of the samples were measured using a Mitutoyo micrometer and laboratory balance with resolutions of 0.001 µm and 0.001 g, respectively. Material removal was evaluated based on the Preston's equation (1):

$$\frac{\Delta H}{\Delta t} = k \cdot p \cdot v \tag{1}$$

where:

ΔH – material removal;
Δt – lapping time;
k – Preston constant;
p – nominal pressure;
v – relative velocity.

The surface quality of the ceramic workpieces was evaluated with the use of a contact profiler, HOMMEL TESTER T500, according to the DIN4777 standard (Ra and Wa parameters), as well as a non-contact 3D optical profilometer, Sensofar S neox, according to the ISO 25178 standard (Sa and Sq parameters, surface topography). Moreover, as shown in Fig. 3 of the measurement setup, a 3D optical profilometer allowed for continuous measurements along the radius of individual segments printed by the SLS method, and considered different contact areas—Fig. 4 based on which tool wear was evaluated. The collected measurement data were then analyzed in dedicated SensoMAP Premium 9.1 software.

4. Experimental results

4.1. Wear characteristics

The effect of process parameters on the wear characteristics of SLS-printed polyamide lapping tools was assessed based on the measurement results obtained from the radial axis of lapping segments. The Sensofar S neox 3D optical profilometer was used to assess the tool's condition based on the surface height profile along its radial axis.

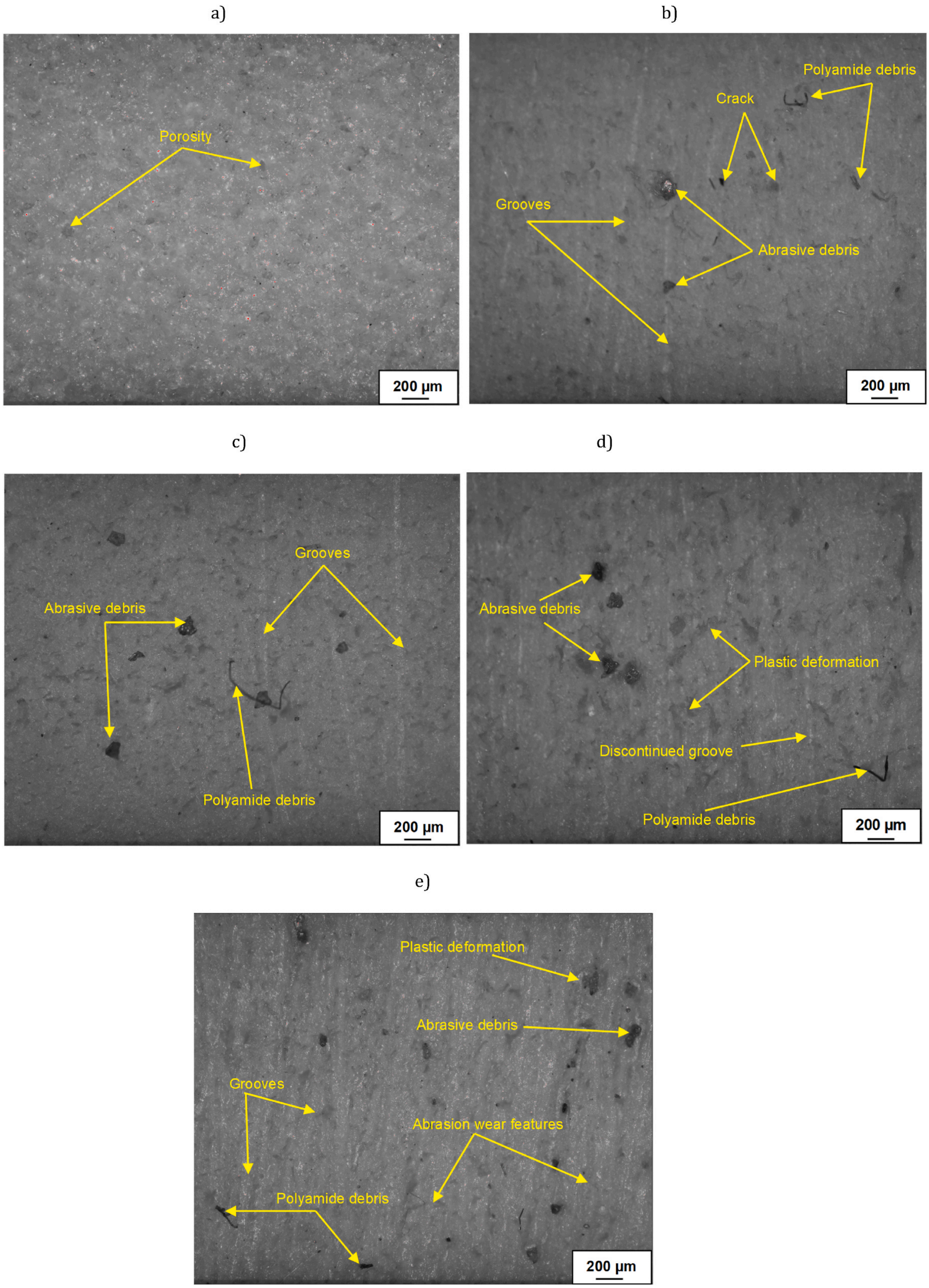

Fig. 12. Surface morphology of an exemplary lapping tools segment #8: a) non-contact region b) radius point 85 mm for p-v-, c) radius point 85 mm for p-v+, d) radius point 85 mm for p+v-, e) radius point 85 mm for p+v+.

Table 3
Statistical plan matrix with averaged measurement results of machining effects.

Machining test no.	Input variable			Output variable			
	$x_1 = p$ [kPa]	$x_2 = v$ [m/s]	$x_3 = t$ [min]	*Δm* [g]	*Δh* [mm]	*Ra* [μm]	*Wa* [μm]
1	6 lower level (−)	0.72 lower level (−)	60 lower level (−)	0.5	0.165	0.54	0.31
2	12 upper level (+)	0.72 lower level (−)	60 lower level (−)	1.069	0.343	0.56	0.27
3	6 lower level (−)	1.44 upper level (+)	60 lower level (−)	1.162	0.375	0.64	0.33
4	12 upper level (+)	1.44 upper level (+)	60 lower level (−)	2.038	0.639	0.5	0.37
5	6 lower level (−)	0.72 lower level (−)	120 upper level (+)	1.096	0.351	0.55	0.32
6	12 upper level (+)	0.72 lower level (−)	120 upper level (+)	2.18	0.682	0.57	0.22
7	6 lower level (−)	1.44 upper level (+)	120 upper level (+)	2.336	0.732	0.57	0.21
8	12 upper level (+)	1.44 upper level (+)	120 upper level (+)	3.487	1.071	0.45	0.47

Measurements are performed on the lapping tool segment with a total length of 120 mm, starting radius 55 mm–175 mm, which includes both contact and non-contact points during machining. By utilizing minimum zone (MZ) methods along the active contact length of the segments, the wear characteristics of each lapping tool were determined based on the extracted waviness profile along the radius of the tool, 65 mm–165 mm.

Apart from the kinematics conditions, the lapping tools wear characteristics depends on the contact density of the workpiece with the lapping tool flat surface. The effect of machining parametric settings on the tool's wear characteristics was assessed using the maximum height of the lapping plate along the tools' contact length, as indicated in Table B.1 of Appendix B. The machining parameters are resulted on the occurrence of varied amount of maximum height along the tools radial axis. Experiments employing parameters p-v- resulted in a maximum height value of 50.95 μm along the tool's active contact length, as shown in Fig. 5. As seen in Fig. 6, the parametric configuration of p-v+ leads to higher values of the tool's maximum height, measuring 60.42 μm. Similarly, Fig. 7 shows a maximum height of 82.41 μm along the tool's contact length with the parametric setting of p+v-. Experiments are being conducted with a parametric setup of p+v+ to ascertain the effect of lapping parameters for long-lasting machining based on the acquired results and the same region of highest contact density along the radial axis of lapping tools. Fig. 8 shows that after 840 min of machining, the maximum height of the lapping segments was 178.16 μm. However, due to the identical lapping kinematics configuration, the parametric settings utilized in this study resulted in a variation of maximum height values on the tool profile, but the same highest contact locations were observed for all parametric settings on the tool's surface over the tool radius of 85 mm.

The parametric maximum height values of the polyamide lapping tool segments, illustrated in Fig. 9, are measurement results for the condition of the eight lapping segments flat surface after machining of ceramic material Al_2O_3 with various parametric settings. In comparison to the other parametric settings, machining the ceramic materials with parametric setting p+v+ produced higher maximum height values in each segment of the four lapping plates where the measurement was performed. This suggests that parametric setting p+v+ causes the occurrence of more wear along the lapping plate's contact length. The results obtained from each segment determine the lapping tool's overall conditions. As shown in Fig. 10, the tool's average maximum height values determine the overall wear characteristics of the tools for various parametric settings. The measured findings demonstrated that machining with a lower parametric setting yields a lower average maximum height, whereas machining with a higher parametric setting yields a greater average maximum height along the tool radius. The lapping plate had the lowest average maximum height with the parametric setting of p-v- and the highest with the parametric setting of p+v+. The average maximum height values for p-v+ and p+v-parametric settings were moderate between values for p-v- and p+v+. The results showed that lapping of ceramic materials with a higher parametric setting results in the occurrence of more wear on the polyamide lapping plates, whereas machining with a lower setting causes less wear on the tool surface.

4.2. Surface topography and morphology of the tools

The tools condition assessments were conducted using a SENSOFAR S neox 3D optical profilometer with a 20X magnification scale after 120 min of machining the ceramic materials Al_2O_3. The assessments were conducted based on the topography of the polyamide lapping segments and surface height distribution along the tool's contact areas. The surface topography at specific radial points of the tool segments was examined using an exemplary lapping segment #8; radius point 85 mm is utilized for the highest contact areas for all parametric settings, and radius point 55 mm is used for the topography measurement of non-contact areas. The non-contact area surface height parameter at radial point 55 mm was determined to have a maximum height (Sz) of 96.76 μm, skewness (Ssk) of −0.05, kurtosis (Sku) of 2.70, and a spatial roughness (Sa) of 12.37 μm, as shown in Fig. 11a. As seen in Fig. 11b, the surface height for parametric setting p-v- indicated the maximum height at 100.86 μm, skewness at −0.05, kurtosis at 6.17, and the spatial roughness at 6.64 μm. As illustrated in Fig. 11c, the parametric setting p-v+ resulted in a spatial roughness of 6.03 μm, skewness of 4.59, kurtosis of 42.59, and a maximum height of 149.29 μm. Using the parametric settings of p+v-, the lapping segment revealed a maximum height of 154.97 μm, skewness of 2.44, kurtosis of 14.78, and a spatial roughness of 9.69 μm, as illustrated in Fig. 11d. The surface height distribution on the segment with parametric settings of p+v+ was found with spatial roughness of 10.84 μm, skewness of 1.73, kurtosis of 12.48, and 202.90 μm of maximum height as shown in Fig. 11e. As presented, the maximum heights on the segments were observed along the radial point with the highest contact, and it's increasing with the higher parametric settings of the lapping setup. Additionally, the measured results of surface height distribution such as skewness and kurtosis for the non-contact region revealed the tool surface was relatively flat, free of extreme peaks or valley features, and with more uniform surface height distribution (since $Sku<3$ and $Ssk \approx 0$). Whereas, for all parametric settings, a radius 85 mm resulted in $Ssk>0$ and $Sku>3$, which implies the surface characteristics of polyamide tool after lapping ceramic samples have been changed and most of the tool's surface heights are distributed below the mean plane and are non-uniform, and sharp peaks extend above the mean plane. This indicates the three-body abrasion lead to a removal of materials from the valleys of polyamide lapping tool's active surface, with highest removal at the highest contact region. Overall, the observed results indicate that lapping of ceramic materials with higher machining parameters p+v+ results in the occurrence of a higher wear on the tool surface while comparing to the rest of the parametric settings.

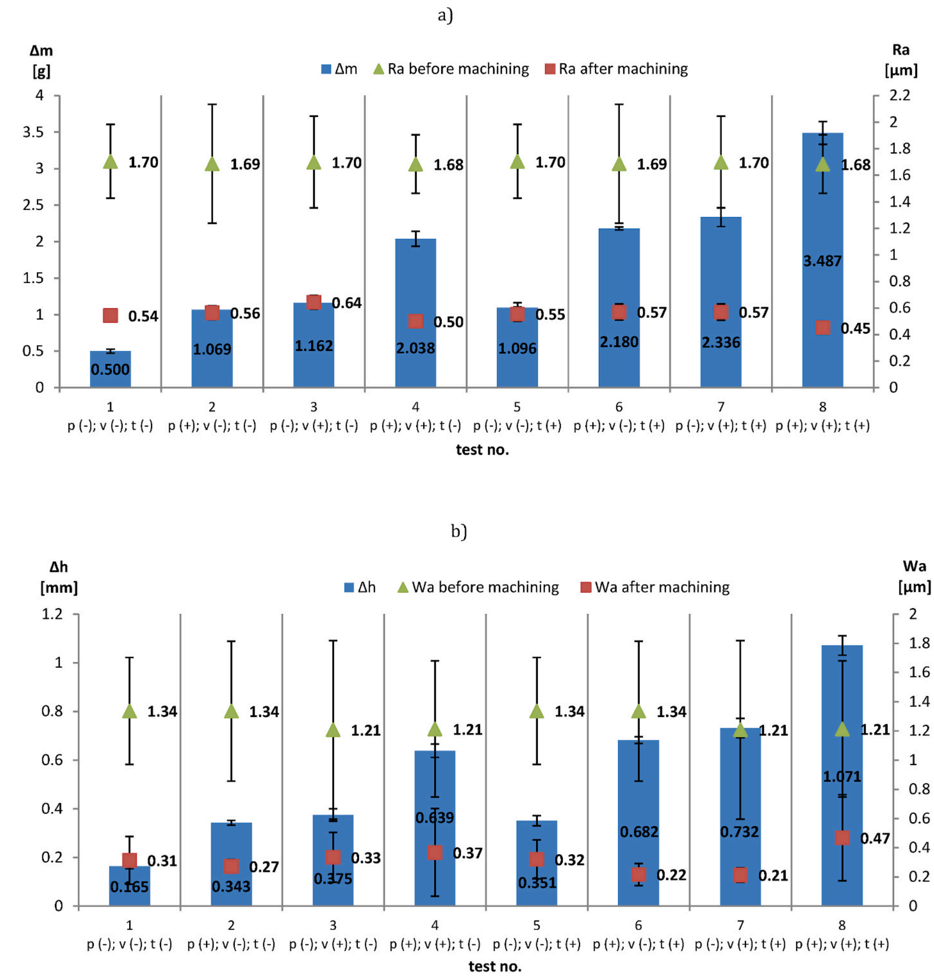

Fig. 13. Technological effects obtained in particular machining tests: a) mass material loss *Δm* and surface roughness Ra; b) linear material loss *Δh* and surface waviness Wa; error bars display ± the standard deviation.

The non-homogenous structure caused by the porosity and roughness of SLS-printed parts and the way AM is made changes the surface characteristics and the way 3D-printed polyamide lapping tools wear and behave [40]. Based on microscopic observations evaluation on wear mechanism of polyamide lapping tools have been conducted considering the non-contact and highest contact regions along the radial axis. As seen from Fig. 12, due to the three-body abrasion of free abrasive lapping process, the wear characteristics of polyamide lapping tools mainly arises from the interaction of ceramics, diamond abrasives, and polyamide tool. However, lapping parameters such as unit pressure and velocity of the lapping process can cause the occurrence of different wear features on the tool active surface. Due to the nature of SLS-printing process, lapping tools fabricated using polyamide powder materials are characterized with a porous surface structure-Fig. 12a, which caused the transition of three-body abrasion into two-body abrasion resulting in effective machining of ceramics. The loose diamond grains' embedment and sliding between the two surfaces result in polyamide lapping tools being worn predominantly due to an abrasion wear mechanism; this is evident from the grooves and scratches on the worn surface as shown in Fig. 12b–e. However, due to the applied load the material flow caused by the plastic deformation can be observed in specific regions. Moreover, larger abrasive particle embedment was seen during lapping with a (p-v-) parametric setting (Fig. 12b); conversely, fine diamond grain embedment was seen during machining with the highest parametric setting, i.e. (p+v+) (Fig. 12e). Generally, the abrasion due to the three-body interaction and the cyclic load causing plastic deformation was seen mainly influencing to worn the active surface of SLS-printed polyamide lapping tools.

4.3. Technological effects

Table 3 provides the developed *PS/DK* 2^3 plan matrix along with the averaged measurement results of the analyzed technological effects. In addition, the results obtained in the particular machining tests are presented in Fig. 13, whereas interaction diagrams in the form of extreme averages for individual outputs are in Fig. 14.

Each of the conducted machining tests was characterized by a stable process, enabling the cutting of ceramics. As expected, significantly the highest values of material loss were obtained with the upper levels (+) of the input variables, i.e., unit pressure $p = 12$ kPa, velocity $v = 1.44$ m/s, and machining time $t = 120$ min—test no. 8, while the lowest values were obtained with the lower levels (−) of variability, i.e., unit pressure $p = 6$ kPa, velocity $v = 0.72$ m/s, and machining time $t = 60$ min—test no. 1. According to Preston's equation (1), increasing the values of unit pressure and machining velocity, as well as extending the machining time, resulted in an increase in material loss—Figs. 13 and 14a and b. As a result of machining after each test, a significant reduction in the values of the surface roughness and waviness parameters of the Al_2O_3 samples was also obtained. The initial average parameter values of Ra = 1.69 μm and Wa = 1.28 μm were reduced to an average level of Ra = 0.55 μm and Wa = 0.31 μm after machining. In contrast to the values of mass and linear material loss, the change of individual levels of input variables did not cause marked differences in the values of the final parameters of roughness Ra and waviness Wa, which was due to the characteristic

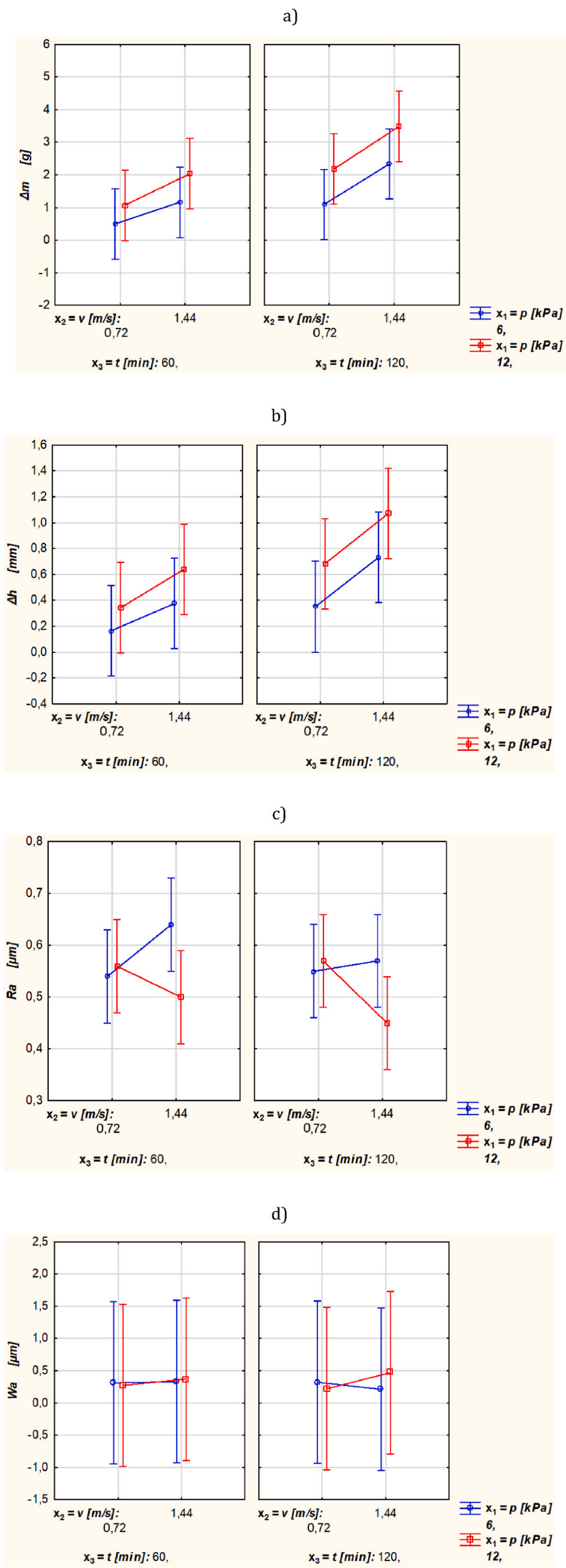

Fig. 14. Interaction diagrams for the analyzed machining results: a) mass material loss *Δm*; b) linear material loss *Δh*; c) surface roughness Ra and d) surface waviness Wa; error bars display ± the standard deviation.

porous structure of ceramics—Figs. 13 and 14c and d. The adopted set of parameters for test no. 8 (unit pressure $p = 12$ kPa, velocity $v = 1.44$ m/s, and machining time $t = 120$ min) resulted in the lowest value of the Ra parameter and a simultaneous increase in the value of the Wa surface waviness parameter compared to previous tests. High values of kinematic parameters and unit pressure affected the increased wear of the lapping plate. Further evaluation of the geometric structure of the surface of the samples was performed on a 3D optical profilometer using the confocal technique with 20x magnification, which indicated a clear smoothing of the surface after each test, as evidenced by the obtained values of the final height parameters Sa and Sq (Fig. 15), as well as the surface topographies of the example samples in Fig. 16. Similar to the 2D measurements based on the Ra parameter, the adopted set of parameters for test no. 8 resulted in a surface with the highest smoothing and characterized by the lowest parameters of Sa = 0.66 μm and Sq = 0.90 μm compared to the other machining tests. Thus, the realization of the lapping process at the values of the analyzed parameters, such as unit pressure $p = 12$ kPa, velocity $v = 1.44$ m/s, and machining time $t = 120$ min, enabled efficient machining and a clear improvement of the surface quality of ceramic workpieces.

4.4. Technological effects modelling

4.4.1. Regression equations for determining the technological effects

Based on the obtained technological effects of one-sided lapping presented in subsection 4.2 and using the *Design of Experiments* module in Statistica software, mathematical models of the analyzed output quantities of the process were developed. Due to the use of a two-level plan and considering the results of previous studies given in paper [13], a linear character of the influence of input quantities on the obtained machining results was assumed. Therefore, mathematical models are functions of three variables in the form $y = f(p, v, t)$. According to the procedure presented in Fig. 2, the first step is assessing the statistical significance of input variables (main effects) and their interactions with the outputs. Figs. 17 and 18 provide the results of the analysis in graphical form based on Pareto plots.

The vertical red line indicated in each of the graphs in Figs. 17 and 18 indicates the critical value of the *t-test* for assessing the statistical significance of the effects of individual factors on the output variables. Crossing this line indicates a statistically significant impact at the assumed confidence level of 95 %. For the amount of material losses of mass *Δm* and linear *Δh*, only main effects significantly affected the obtained results. Meanwhile, the interaction of unit pressure *p* and lapping velocity *v* interacted significantly with the value of the roughness parameter Ra, while the effect of unit pressure *p* alone was relatively pronounced. The analysis also indicated that there was no significant statistical effect of individual factors and their interactions on the value of the Wa parameter. Thus, statistical analysis indicated a significant influence of main effects and a negligible influence of their interaction for material losses and only a statistically significant influence of the interaction of unit pressure *p* and lapping velocity *v* for the Ra parameter. Therefore, the mathematical models developed for material losses omitted the interaction components, whereas only the interaction of two factors was considered for the Ra parameter. Finally, the regression coefficients determined in the software and the mathematical models (regression functions) are presented in the form of linear equations (2)–(4):

$$\Delta m = -2.837 + 0.15333{*}p + 1.45069{*}v + 0.01804{*}t \tag{2}$$

$$\Delta h = -0.8435 + 0.046333{*}p + 0.443056{*}v + 0.005475{*}t \tag{3}$$

$$Ra = 0.615 - 0.006944{*}p{*}v \tag{4}$$

Moreover, Figs. D.1–D.3 presented in Appendix D shows the response planes for the developed models of technological effects at a constant value of the specified variable and the formula of the fitted function.

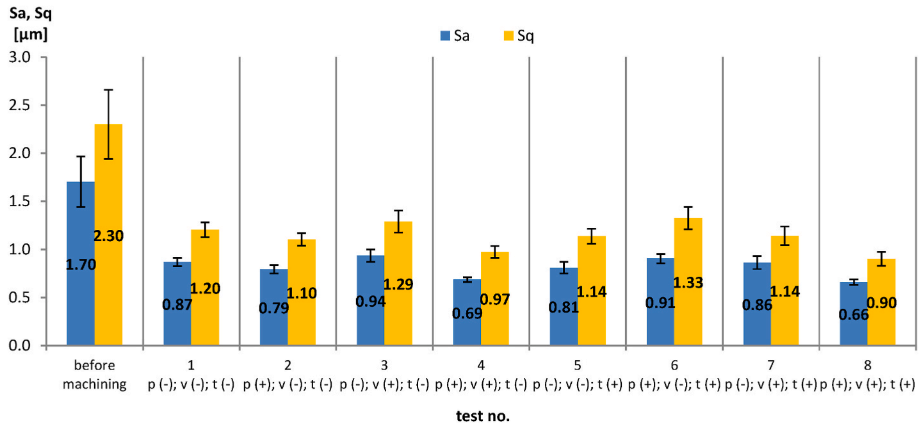

Fig. 15. Average values of Sa and Sq height parameters obtained in particular machining tests; error bars display ± the standard deviation.

4.4.2. Evaluation and validation of regression equations

In the last step, the determined regression equations of the analyzed technological effects were evaluated and validated. For this purpose, the results of measurements from subsequent machining tests were compared with predicted values calculated using mathematical models described by equations (2)–(4). The quality of fit of each linear function to the experimental data was evaluated using the coefficient of determination R^2 according to equation (Eq. (A.1). In addition, absolute Δy, relative δ errors, and the root mean squared error *RMSE* were determined using the equations (Eq. (A.2), (Eq. (A.3), and equation (Eq. (A.4) respectively as presented in Appendix A.

Measurement data obtained after 60 min and 120 min of machining were used to evaluate the mathematical models, which resulted from the adopted experimental plan. However, additional data obtained from measurements conducted after 80 min and 100 min of machining were used to validate the mathematical models. A comparison of results for the analyzed technological effects are presented in Tables C.1–C4 of Appendix C and in Figs. E.1–E.3 of Appendix E.

The conducted evaluation and validation of mathematical models using selected coefficients indicated the occurrence of relatively small differences between measured and predicted values using the determined regression equations. The value of the coefficient of determination, $R2 = 0.97$, for material loss confirms the high fit of the proposed regression equations to the experimental data. Thus, mathematical models explain 97 % of the variability in results. The validation conducted using additional data also confirmed the occurrence of small differences between measured and calculated values using mathematical models. The highest values of determined errors occurred for the lower levels of input parameters of the machining process ($p = 6$ kPa and $v = 0.72$ m/s) – (Table C.1 of Appendix C, Fig. E.1a, and Fig. E.2a of Appendix E), which resulted from the tool reinforcement mechanism and the character of the abrasive grains work. Relatively low values of the indicated process parameters and machining time did not result in effective reinforcement of the tool with diamond grains, thus indicating the dominant influence of 3-body abrasive wear. Meanwhile, increasing the value of unit pressure p and cutting speed v for subsequent tests influenced more intense penetration of diamond grains into the plastic structure of the tools and, consequently, enabled much more efficient cutting, similar to grinding or grinding with lapping kinematics using electroplated tools. In addition, the values of the analyzed errors decreased significantly for subsequent setups—refer Fig. E.3 of Appendix E. In the case of the regression equation describing the roughness parameter *Ra*, the determined value of the coefficient $R^2 = 0.4$ is significantly lower compared to material loss models. This is due to the inclusion of only one statistically significant interaction *pv* in the regression function and the rejection of the other main effects and their interactions. Despite this, the measured values are strongly close to those predicted using the designated model. In addition, due to the characteristic porous structure of ceramic workpieces, similar final values of the roughness parameter *Ra* were obtained for each set of analyzed parameters. In conclusion, the obtained results indicated the possibility of practical use of the proposed regression equations for further research and implementation work.

5. Discussion

The conducted systematic machining tests using SLS-printed wheels confirmed previous findings given in papers [13,40] regarding the possibility of using this type of tool and a type of abrasive suspension containing loose diamond *D107* grains in the efficient abrasive machining of difficult-to-cut materials such as advanced ceramic materials. A clear influence of the analyzed and crucial lapping parameters, such as unit pressure p, velocity v, and machining time t, on the obtained technological effects and wear characteristics of SLS-printed tools was observed. According to Preston's equation (1), increasing the unit pressure p, the cutting speed v, and extending the machining time t resulted in an increase in the material loss values of the Al_2O_3 samples, without a significant effect on the final values of the roughness parameters. Thus, the adopted set of parameters for machining test no. 8 (unit pressure $p = 12$ kPa, velocity $v = 1.44$ m/s, and machining time $t = 120$ min) were observed, enabling the most efficient performance of the machining process. According to observations of the active surface of the tools demonstrated in papers [13], the use of the indicated and relatively high unit pressure p and cutting speed v enabled the tools to be effectively reinforced with abrasive grains that were partially embedded in the structure of the flexible plate made of polyamide PA2200 at the level of ~50 % of their height. The change in the values of the analyzed factors directly affected the nature of the work of the abrasive grains in the abrasive suspension, which further influenced the values of material loss of the samples and wear of the lapping wheel. The observed significantly lower material loss from the test with the lower parameter values (unit pressure $p = 6$ kPa, velocity $v = 0.72$ m/s) may indicate the dominant character of 3-body abrasion, during which the abrasive grains mainly rolled between the surfaces of the samples and the tool and partially penetrated the elastic structure of the wheel. When the values of the indicated parameters increased, there was more intensive penetration of the grains into the tool surface, indicating the dominant character of 2-body abrasion, similarly to the grinding and grinding with lapping kinematics. The effect of process parameters on the wear characteristics of SLS-printed polyamide lapping plates was investigated, and the results showed that machining with higher parametric settings can result in more wear on the tool's surface, which is confirmed by profilometer observation of the lapping tool's radial axis profile, as well as surface topography measurements. The findings also revealed that the tool's radius point of 85 mm has the highest contact position throughout the radial length for all parametric settings, which is expected to be the

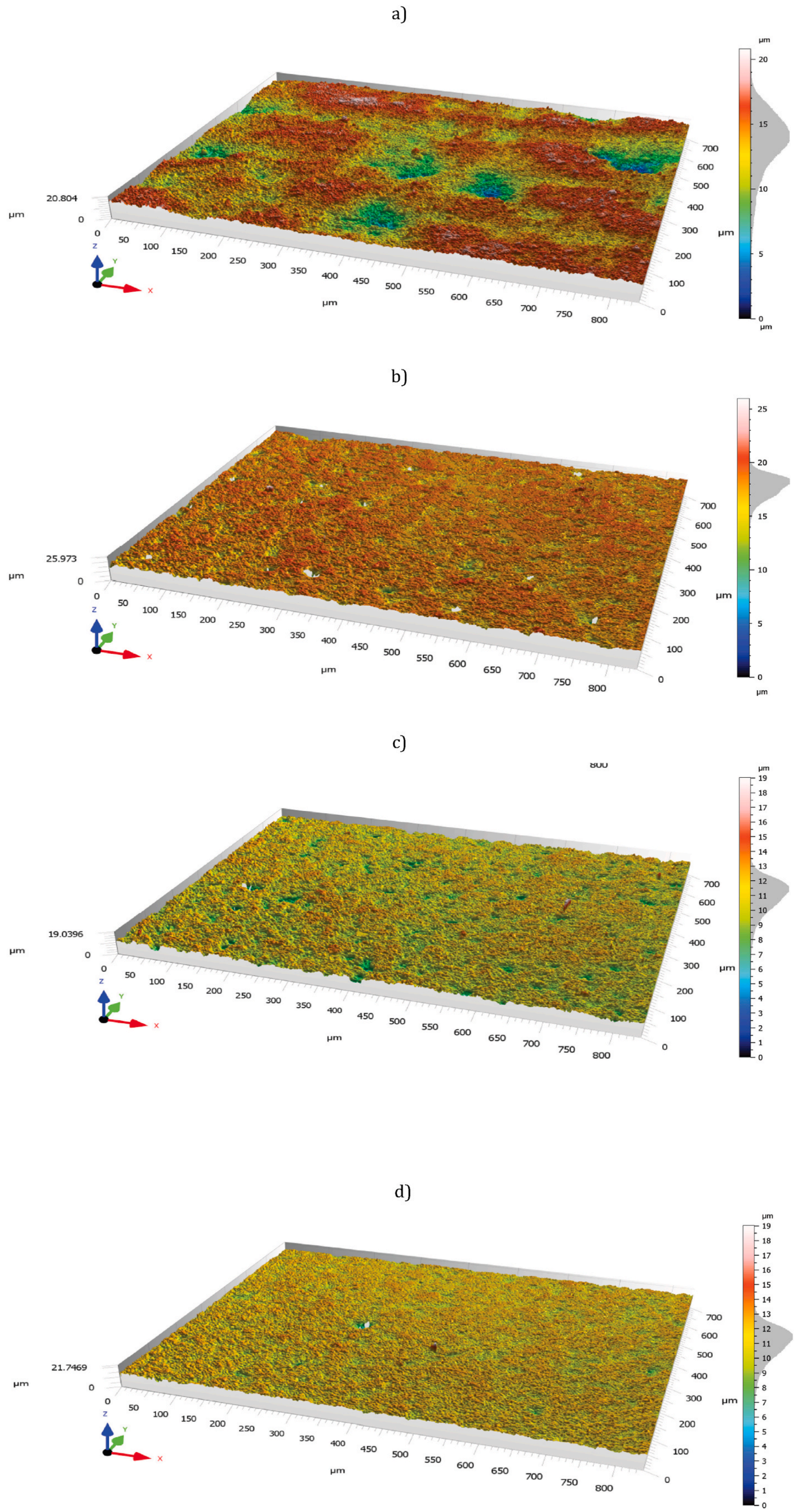

Fig. 16. Selected surface topographies of ceramic workpieces: a) before machining; b) after test no. 6 (p = 12 kPa, v = 0.72 m/s, t = 120 min); c) after test no. 7 (p = 6 kPa, v = 1.44 m/s, t = 120 min) and d) after test no. 8 (p = 12 kPa, v = 1.44 m/s, t = 120 min).

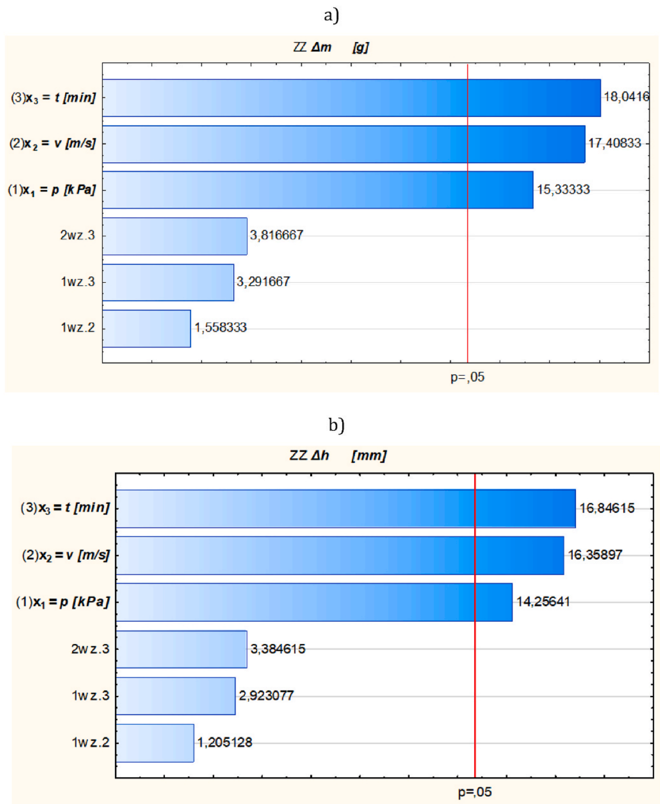

Fig. 17. Pareto plots of the effects of standardized input quantities and their interactions for material loss: a) mass Δm; b) linear Δh.

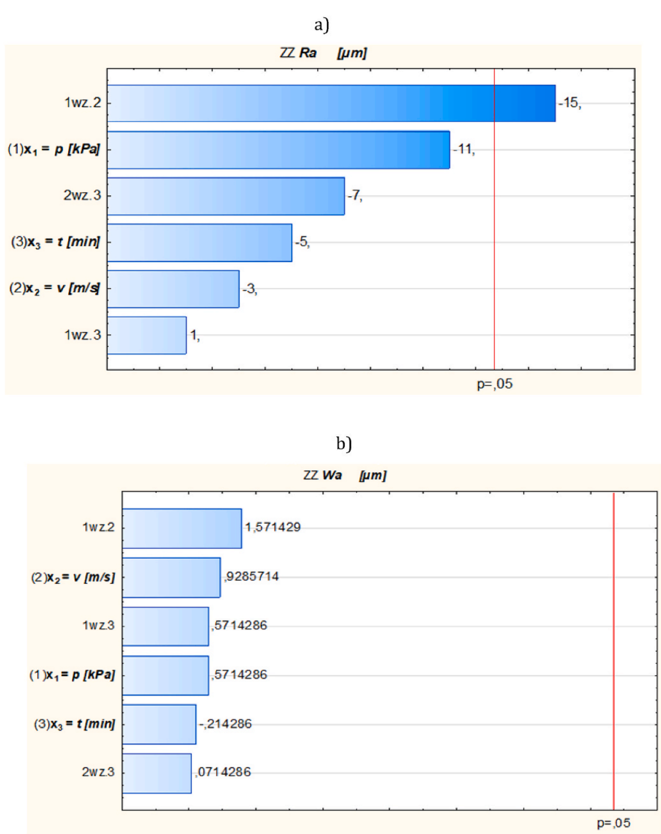

Fig. 18. Pareto plots of the effects of standardized input quantities and their interactions for surface roughness and waviness parameters: a) Ra; b) Wa.

area with the most wear. These findings are also supported by investigations conducted using simulation [41] and combined simulation and experimental assessments [42]. In addition, the results of statistical evaluation, which are given in Fig. D.1 of Appendix D, indicated a significant influence of the analyzed main factors on the material removal. Therefore, the regression equations for material losses mass Δm and linear Δh include all analyzed factors *p, v,* and *t* as statistically significant. After each of the machining tests performed, there was a clear improvement in the surface quality of the ceramics. At the same time, changing the particular values of the input factors did not affect the final values of the 2D and 3D surface roughness parameters of the Al_2O_3 samples. This was also confirmed by the results of the statistical significance evaluation and the inclusion of only one statistically significant interaction *pv* in the regression equation of the roughness parameter *Ra*. However, similar roughness parameter values after each machining test were obtained due to the characteristic porous structure of the ceramic material Al_2O_3.

6. Conclusions and future works

The effect of lapping parameters on the wear characteristics and performance of SLS-printed polyamide lapping tools have been experimentally assessed for single-sided free abrasive machining of ceramic materials, Al_2O_3. Experimental investigations were conducted by considering parameters with two levels, such as unit pressure *(p)*, velocity *(v)*, and machining time (t), and applying the *PS/DK* 2^3 statistical plans. Based on minimum zone methods (MZ) and topographical observations, 3D-printed lapping tools wear assessment has been carried out along the radial length of the tools active surface. Technological effects of the process have been evaluated to determine the effects of parametric settings within the specified ranges, and the most important conclusions from the research are drawn as follows.

- The parametric setting p+v+ resulted in a higher maximum height along the radial length of polyamide lapping segments. This indicates that parametric settings having higher values result in the occurrence of bigger tool wear while comparing to the parametric settings with lower values. Additionally, due to the ideal executed co-rotational kinematic configurations during the experiments, the highest contact density along the radial length of the tools was found on the radius of 85 mm for all parametric settings. Due to this highest contact density along the radial axis of the tool surface, a radial point of 85 mm can be expected with bigger tool wear. However, the prototype abrasive tools were characterized by relatively low wear.
- Changing the process input factors, such as unit pressure *p*, velocity v, and machining time *t,* significantly influences technological aspects of the machining, mainly the values of material losses and wear characteristics of SLS-printed tools. Machining with upper values of parameters such as unit pressure $p = 12$ kPa, velocity $v = 1.44$ m/s, and machining time $t = 120$ min resulted in the highest values of mass material losses $\Delta m = 3.49$ g and linear $\Delta h = 1.07$ mm, as well as the lowest values of roughness parameters Ra = 0.45 μm, Sa = 0.66 μm, and Sq = 0.9 μm.
- After each test, a significant improvement in surface quality was observed, as confirmed by the values of the analyzed roughness parameters and surface topographies. A similar roughness parameter values of Ra ~0.55 μm, Sa ~0.82 μm, and Sq ~1.13 μm was obtained due to the characteristic porous structure of the machined ceramics.
- The developed mathematical models in the form of regression equations can be used to precisely predict the values of the output quantities within the specified range of variation of the machining parameters. This is evidenced by the small values of the calculated errors. Based on statistical significance evaluation, the mathematical models for material losses mass Δm and linear Δh include the main effects *p, v, and t*, while the mathematical model for the roughness parameter *Ra* includes only the interaction of *p* and *v*.

- Lapping with the use of SLS-printed tools with machining parameters $p = 12$ kPa, $v = 1.44$ m/s, and $t = 120$ min enables an efficient and stable process, which is confirmed both by the obtained experimental results and the data defining the fit of the measured values to the predicted values using the proposed regression equations.

Generally, results from the investigations unveiled the effects of process parameters on SLS-printed lapping plates, indicating locations for bigger tool wear on tool surfaces and determining the influential parametric settings from the specified range. However, the 3D-printed polyamide lapping plates resulted in efficient material removal and significant improvement of the ceramic material Al_2O_3 surface quality with the occurrence of lower wear on the tools surfaces. Future work will focus on developing more accurate and advanced models for the selected technological effects and tool wear. This can be conducted based on the data collected as a result of process performance with different parameters. Based on this, general guidelines for the selection of an appropriate set of parameters based on the types of materials can be defined. Additionally, further study on the optimization of SLS 3D printing parameters will enhance the wear resistance and performance of polyamide lapping tool.

CRediT authorship contribution statement

Dawid Zieliński: Writing – review & editing, Writing – original draft, Validation, Methodology, Investigation, Data curation. **Sisay Workineh Agebo:** Writing – review & editing, Writing – original draft, Validation, Methodology, Investigation, Formal analysis. **Mariusz Deja:** Writing – review & editing, Writing – original draft, Supervision, Methodology, Investigation, Funding acquisition, Formal analysis, Conceptualization.

Declaration of competing interest

The authors declare that they have no known competing financial interests or personal relationships that could have appeared to influence the work reported in this paper.

Acknowledgements

This work is funded by the European Commission in the framework HORIZON-WIDERA-2021-ACCESS-03, project 101079398 'New Approach to Innovative Technologies in Manufacturing (NEPTUN)'.

Appendix A. Evaluation of regression equations

Evaluation and validation of the developed mathematical equations (2)–(4) have been conducted using the coefficient of determination (Eq. (A.1) for the quality of linear function fit to the experimental data. Absolute, relative, and root mean square errors are determined using Eq. (A.2), Eq. (A.3), and Eq. (A.4). The calculated value and comparisons are presented in Table C.1-Table C.4.

$$R^2 = \frac{\sum_{i=1}^{n} (\widehat{y}_i - \overline{y})^2}{\sum_{i=1}^{n} (y_i - \overline{y})^2} \quad \text{(Eq. A.1)}$$

$$\Delta y = |y_i - \widehat{y}_i|, \quad \text{(Eq. A.2)}$$

$$\delta = \left(\frac{|y_i - \widehat{y}_i|}{y_i}\right) 100\%, \quad \text{(Eq. A.3)}$$

$$\text{RMSE} = \sqrt{\frac{1}{n}\sum_{i=1}^{n} (\widehat{y}_i - y_i)^2}, \text{where:} \quad \text{(Eq. A.4)}$$

$\overline{y}$ – arithmetic mean of the real/measured values of the technological effect;
y_i – the measured value of the technological effect;
$\widehat{y}_i$ – the value of the technological effect calculated from the regression equation;
n – the total amount of measurement data.

Appendix B. Measurement of lapping plates surface height parameters

The surface height parameters of Wp and Wv were collected from the waviness profile and used to calculate maximum height along the tools' contact length, as presented in Table B.1. Based on this, the wear characteristics of polyamide lapping tools' were assessed considering the effect of parametric settings. These values correspond to data originally presented in Figs. 9 and 10.

Table B.1
Surface profile measurement results of the lapping plate's maximum height.

Segment no.	Height parameters (Wp, Wv)								Maximum height: Wt (mm)			
	Peak: Wp (mm)				Valley: Wv (mm)							
	p+v+	p+v-	p-v-	p-v+	p+v+	p+v-	p-v-	p-v+	p+v+	p+v-	p-v-	p-v+
1	0.07918	0.02475	0.03477	0.06011	−0.04380	−0.03280	−0.02096	−0.04031	0.12298	0.05755	0.05573	0.10042
2	0.09495	0.03778	0.03444	0.02457	−0.05543	−0.03453	−0.03687	−0.02036	0.15038	0.07231	0.07131	0.04493
3	0.09693	0.03641	0.03382	0.04031	−0.04790	−0.02650	−0.06833	−0.03441	0.14483	0.06291	0.10215	0.07472
4	0.10968	0.04115	0.02518	0.02832	−0.07146	−0.04702	−0.03915	−0.02733	0.18114	0.08817	0.06433	0.05565
5	0.09183	0.05011	0.02680	0.06434	−0.04985	−0.01865	−0.03557	−0.03115	0.14168	0.06876	0.06237	0.09549
6	0.08505	0.03348	0.02645	0.02947	−0.04853	−0.03107	−0.03981	−0.02342	0.13358	0.06455	0.06626	0.05289
7	0.09708	0.05031	0.02954	0.03763	−0.05479	−0.09725	−0.02368	−0.02489	0.15187	0.14756	0.05322	0.06252
8	0.12219	0.04080	0.03595	0.03486	−0.05597	−0.04161	−0.01500	−0.02556	0.17816	0.08241	0.05095	0.06042

Appendix C. Evaluation of experimental data and determination of root mean squared error

Predicted values of technological effects are calculated using the developed regression equations for specified parametric settings and compared with the measured ones. The calculated values of absolute, relative, and root mean square errors are presented in Table C.1-Table C.4. These values correspond to data presented in Figure E.1-Figure E.3.

Table C.1
Comparison of measured and predicted values for $p = 6$ kPa (lower level) and $v = 0.72$ m/s (lower level).

Output variable	Iput variable			Y	$\hat{Y}$	R^2	Values of determined errors		
	$x_1 = p$ [kPa]	$x_2 = v$ [m/s]	$x_3 = t$ [min]				Δy [g/mm/µm]	Δ [%]	*RMSE* [g/mm/µm]
Δm	6	0.72	60	0.500	0.210	0.97	0.290	58.025	0.097
			120	1.096	1.292		0.197	17.944	0.066
			80	0.691	0.571	0.97	0.120	17.413	0.040
			100	0.890	0.931		0.042	4.700	0.014
Δh	6	0.72	60	0.165	0.082	0.97	0.083	50.203	0.028
			120	0.351	0.410		0.060	16.988	0.020
			80	0.226	0.191	0.97	0.035	15.391	0.012
			100	0.288	0.301		0.013	4.513	0.004
Ra	6	0.72	60	0.54	0.59	0.40	0.042	7.669	0.014
			120	0.55	0.59		0.031	5.511	0.010
			80	0.61	0.59	0.40	0.028	4.619	0.009
			100	0.59	0.59		0.001	0.095	0.0002

Table C.2
Comparison of measured and predicted values for $p = 12$ kPa (upper level) and $v = 0.72$ m/s (lower level).

Output variable	Input variable			Y	$\hat{Y}$	R^2	Values of determined errors		
	$x_1 = p$ [kPa]	$x_2 = v$ [m/s]	$x_3 = t$ [min]				Δy [g/mm/µm]	δ [%]	*RMSE* [g/mm/µm]
Δm	12	0.72	60	1069	1.130	0.97	0.061	5.726	0.020
			120	2.180	2.212		0.032	1.464	0.011
			80	1.449	1.491	0.97	0.041	2.851	0.014
			100	1.817	1.851		0.034	1.878	0.011
Δh	12	0.72	60	0.343	0.360	0.97	0.017	5.091	0.006
			120	0.682	0.688		0.006	0.936	0.002
			80	0.461	0.469	0.97	0.009	1.868	0.003
			100	0.571	0.579		0.008	1.440	0.003
Ra	12	0.72	60	0.56	0.56	0.40	0.009	1.673	0.003
			120	0.57	0.56		0.015	2.631	0.005
			80	0.53	0.56	0.40	0.025	4.718	0.008
			100	0.56	0.56		0.004	0.695	0.001

Table C.3
Comparison of measured and predicted values for $p = 6$ kPa (lower level) and $v = 1.44$ m/s (upper level).

Output variable	Iput variable			Y	$\hat{Y}$	R^2	Values of determined errors		
	$x_1 = p$ [kPa]	$x_2 = v$ [m/s]	$x_3 = t$ [min]				Δy [g/mm/µm]	δ [%]	*RMSE* [g/mm/µm]
Δm	6	1.44	60	1.162	1.254	0.97	0.093	7.981	0.031
			120	2.336	2.337		0.0004	0.019	0.0001
			80	1.552	1.615	0.97	0.063	4.070	0.021
			100	1.949	1.976		0.027	1.367	0.009
Δh	6	1.44	60	0.375	0.401	0.97	0.026	7.028	0.009
			120	0.732	0.729		0.002	0.296	0.001
			80	0.494	0.510	0.97	0.016	3.293	0.005
			100	0.615	0.620		0.005	0.795	0.002
Ra	6	1.44	60	0.64	0.56	0.40	0.088	13.730	0.029
			120	0.57	0.56		0.015	2.631	0.005
			80	0.61	0.56	0.40	0.051	8.348	0.017
			100	0.62	0.56		0.065	10.483	0.022

Table C.4
Comparison of measured and predicted values for $p = 12$ kPa (upper level) and $v = 1.44$ m/s (upper level).

Output variable	Input variable			Y	$\hat{Y}$	R^2	Values of determined errors		
	$x_1 = p$ [kPa]	$x_2 = v$ [m/s]	$x_3 = t$ [min]				Δy [g/mm/μm]	δ [%]	*RMSE* [g/mm/μm]
Δm	12	1.44	60	2.038	2.174	0.97	0.136	6.691	0.045
			120	3.487	3.257		0.230	6.603	0.077
			80	2.592	2.535	0.97	0.057	2.206	0.019
			100	3.060	2.896		0.164	5.351	0.055
Δh	12	1.44	60	0.639	0.679	0.97	0.040	6.296	0.013
			120	1.071	1.007		0.063	5.920	0.021
			80	0.804	0.788	0.97	0.015	1.901	0.005
			100	0.945	0.898		0.047	4.940	0.016
Ra	12	1.44	60	0.50	0.50	0.40	0.005	0.998	0.002
			120	0.45	0.50		0.043	9.461	0.014
			80	0.53	0.50	0.40	0.036	6.798	0.012
			100	0.48	0.50		0.011	2.180	0.004

Appendix D. Response surface plots of technological effects

The relations between variables and technological effects are presented in Figure D.1-Figure D.3. These plots can be used to identify the best combinations of input variables to obtain the required technological effects.

a)

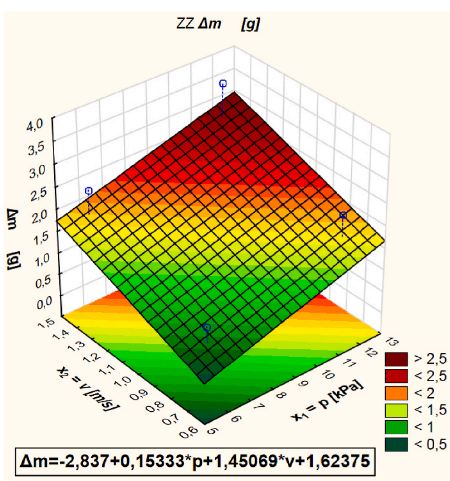

b)

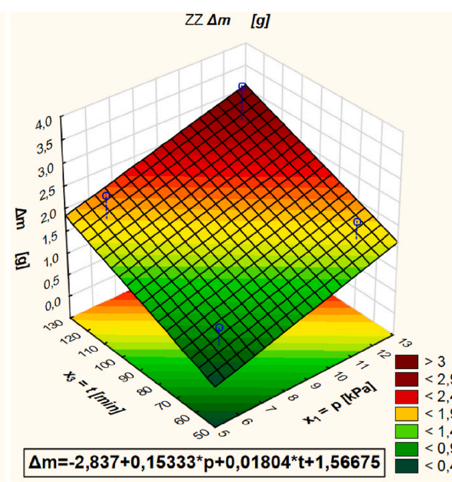

c)

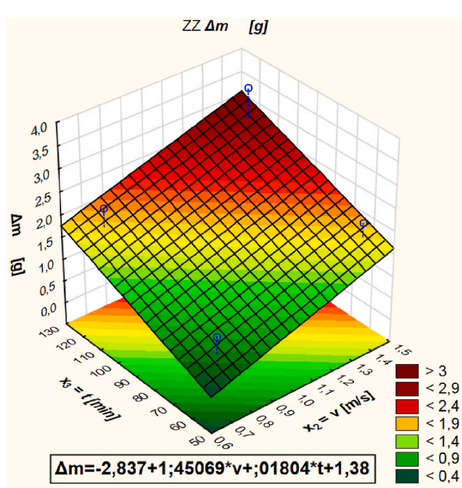

Fig. D.1. Response planes for mass material loss Δm: a) constant value of variable $x_3 = t = 90$ min; b) constant value of the variable $x_2 = v = 1.08$ m/s; c) constant value of the variable $x_1 = p = 9$ kPa.

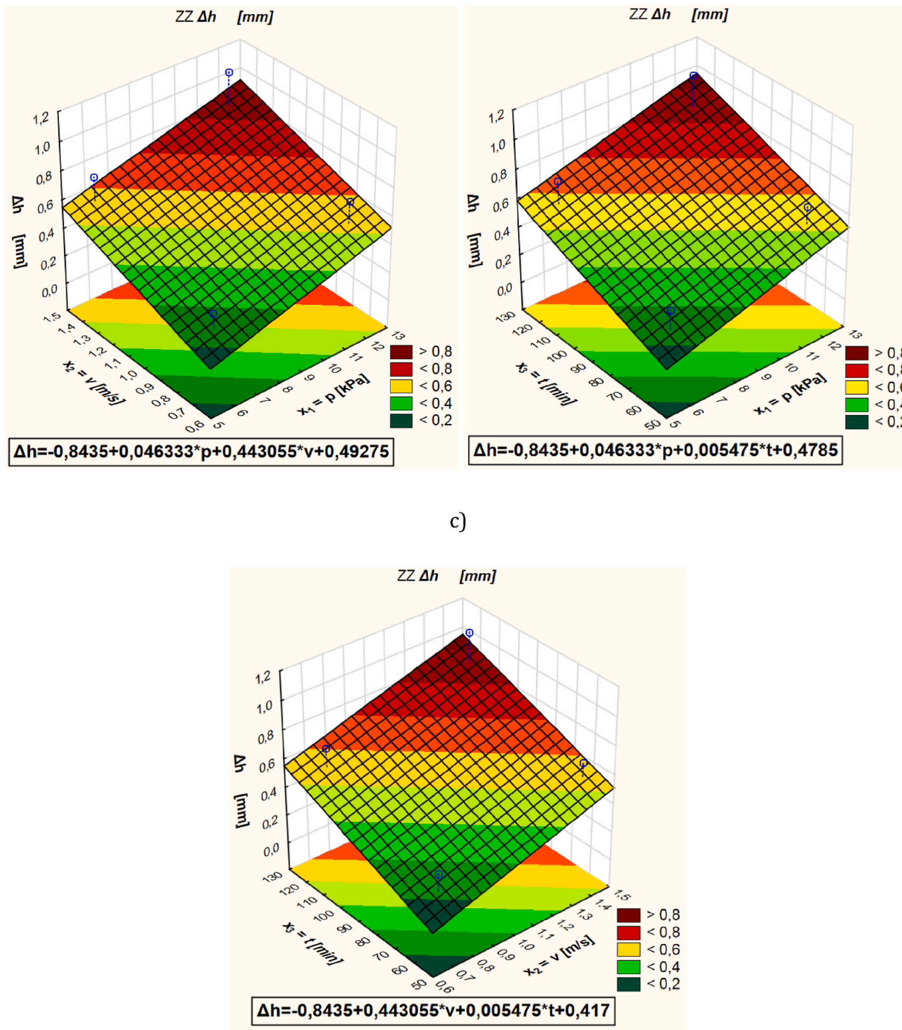

Fig. D.2. Response planes for linear material loss Δh: a) constant value of variable $x_3 = t = 90$ min; b) constant value of the variable $x_2 = v = 1.08$ m/s; c) constant value of the variable $x_1 = p = 9$ kPa.

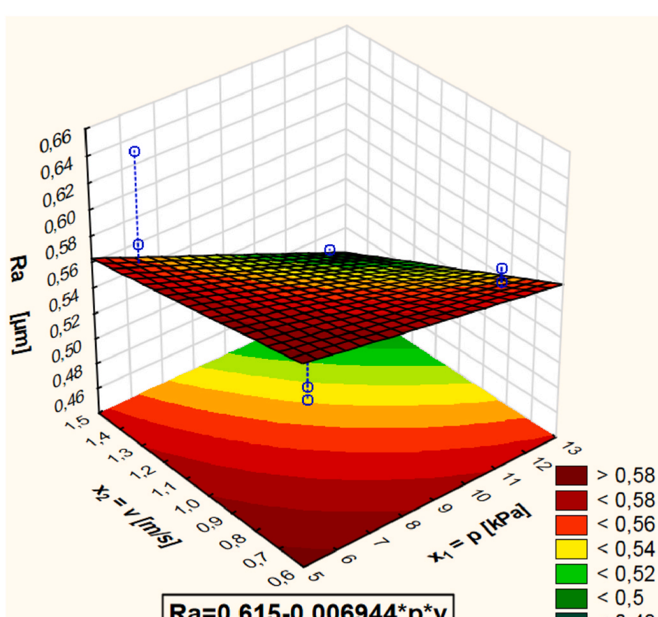

Fig. D.3. Response plane for roughness parameter *Ra*.

Appendix E. Evaluation of measured and predicted values

The measured and predicted values of technological effects within specified parametric settings were used for comparison in the presented Figure E.1-Figure E.3.

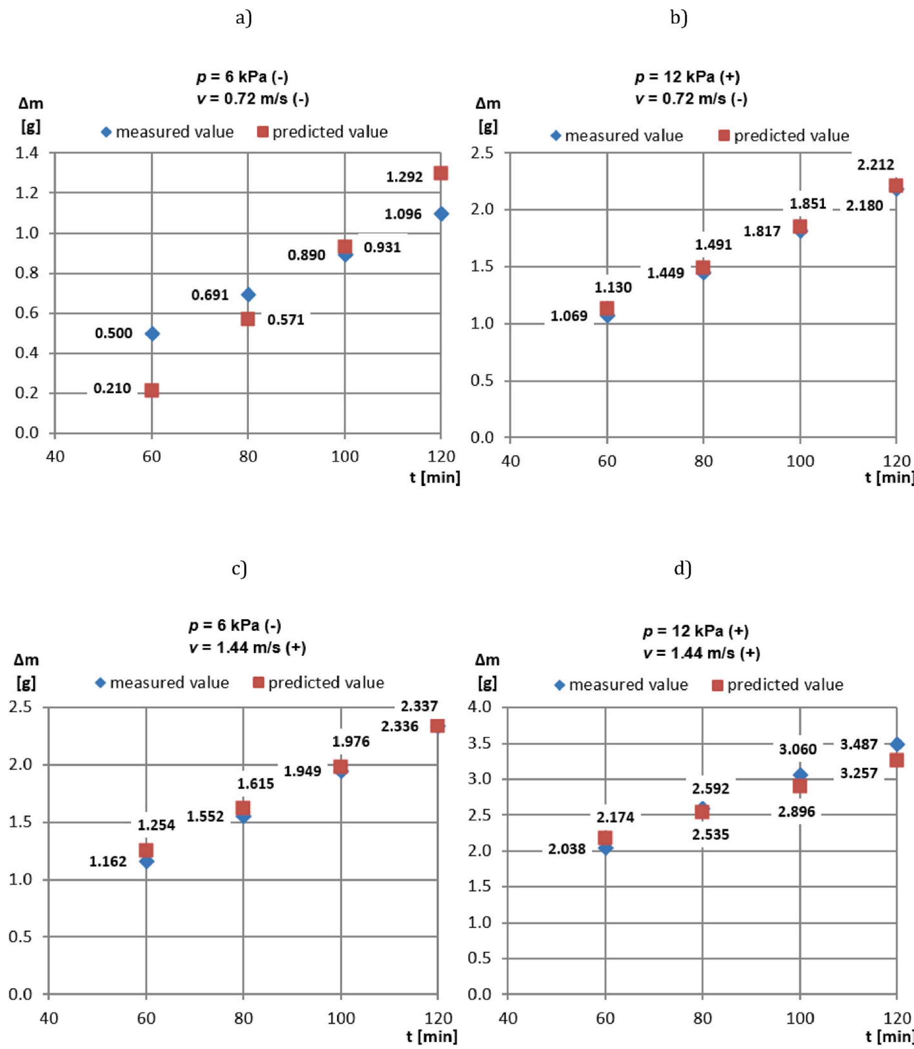

Fig. E.1. Comparison of measured and predicted values for mass material loss Δm.

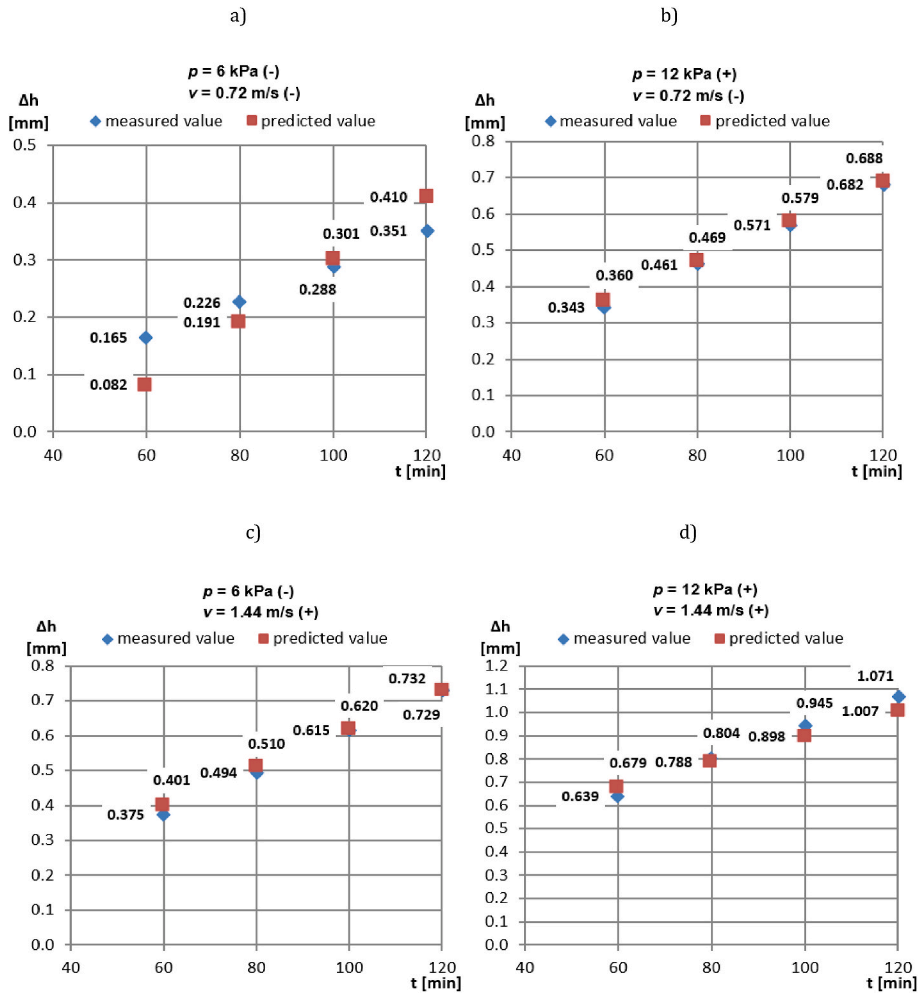

Fig. E.2. Comparison of measured and predicted values for linear material loss Δh.

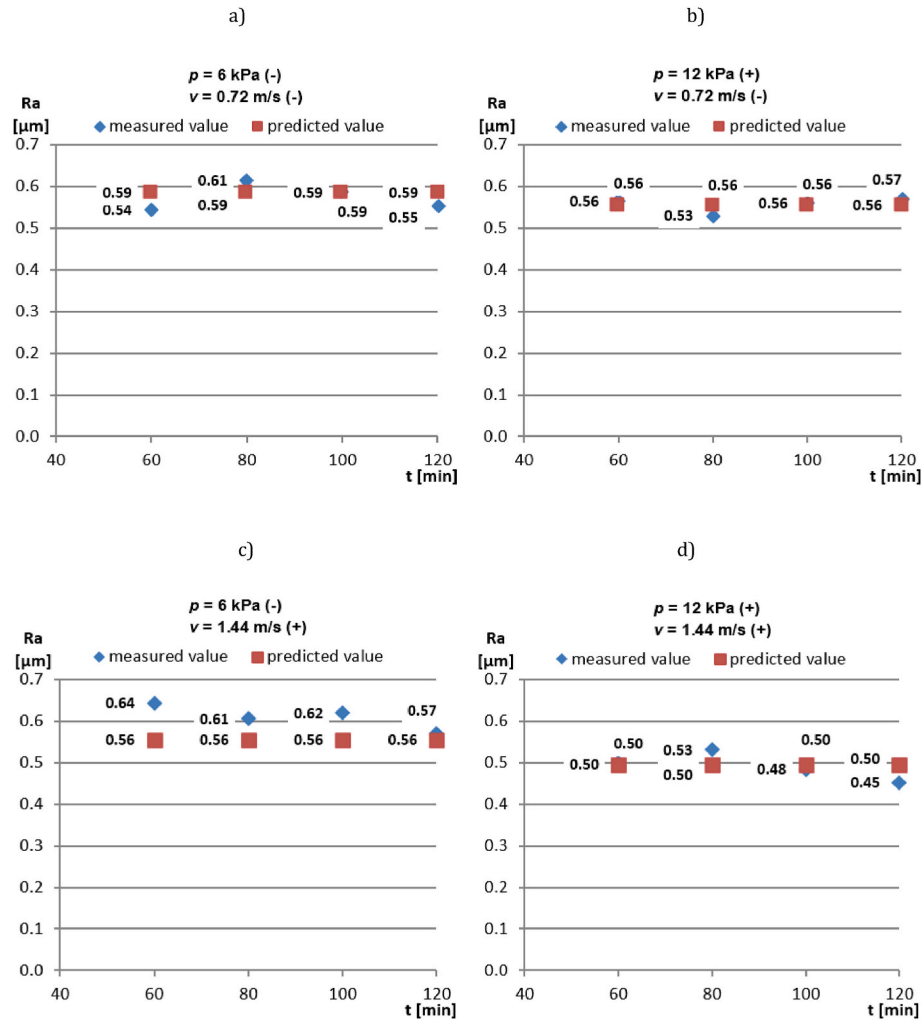

Fig. E.3. Comparison of measured and predicted values for roughness parameter Ra.

Data availability

Data will be made available on request.

References

[1] A. Deaconescu, T. Deaconescu, Experimental and statistical parametric optimisation of surface roughness and machining productivity by lapping, Trans. FAMENA 39 (2015) 65–78.

[2] Z. Hu, et al., Speed ratio optimization for ceramic lapping with fixed diamond pellets, Int. J. Adv. Manuf. Technol. 90 (9–12) (2017) 3159–3169.

[3] U. Satake, et al., Optimization method for double-sided polishing process based on kinematical analysis, Procedia CIRP 41L (2016) 870–874.

[4] M. Sahab Ar, et al., Effect of double sided process parameters in lapping silicon wafer, Appl. Mech. Mater. 393 (2013) 259–265.

[5] E. Uhlmann, T.G. Ardelt, Influence of kinematics on the face grinding process on lapping machines, CIRP Ann. 48 (1999) 281–284.

[6] T. Kasai, et al., Improvement of conventional polishing conditions for obtaining super smooth surfaces of glass and metal works, CIRP Ann 39 (1990) 321–324.

[7] H.Y. Tam, H.B. Cheng, Y.W. Wang, Removal rate and surface roughness in the lapping and polishing of RB-SiC optical components, J. Mater. Process. Technol. 192–193 (2007) 276–280.

[8] D. Zieliński, M. Deja, M. Zator, A comparative study of precision surface grinding using additively fabricated Acrylonitrile–Butadiene–Styrene (ABS) wheels with continuous and serrated working surfaces, Materials 17 23 (2024) 5867, https://doi.org/10.3390/ma17235867.

[9] M. Deja, D. Zieliński, A.Z.A. Kadir, S.N. Humaira, Applications of additively manufactured tools in abrasive machining—a literature review, Materials 14 5 (2021) 1318.

[10] L. Guo, Q. Huang, I. Marinescu, Effect of nanosized alumina fillers on manufacturing of UV light-curable-resin bond abrasive tool, Mach, Sci. Technol. 21 (2017) 223–238.

[11] L. Guo, et al., An experimental study on the abrasive machining process of electronic substrate material with a novel ultraviolet-curable resin bond diamond lapping plate, IEEE Access 7 (2019) 64375–64385.

[12] Z.J. Du, et al., Selective laser sintering and grinding performance of resin bond diamond grinding wheels with arrayed internal cooling holes, Ceram. Int. 45 (2019) 20873–20881.

[13] M. Deja, D. Zieliński, A pilot study on machining difficult-to-cut materials with the use of tools fabricated by SLS technology, Materials 14 (2021) 5306, https://doi.org/10.3390/ma14185306.

[14] F. Molaiekiya, M. Aramesh, S.C. Veldhuis, Chip formation and tribological behaviour in high-speed milling of IN718 with ceramic tools, Wear 446 (2020) 203191.

[15] E. Medvedovski, Wear-resistant engineering ceramics, Wear 249 (9) (2001) 821–828.

[16] P. Pawar, R. Ballav, A. Kumar, An overview of machining process of alumina and alumina ceramic composites, Manuf. Sci. Technol. 3 (1) (2015) 10–15.

[17] K. Poser, K.H. Zum Gahr, J. Schneider, Development of Al_2O_3 based ceramics for dry friction systems, Wear 259 (1–6) (2005) 529–538.

[18] C.W. Chang, C.P. Kuo, Evaluation of surface roughness in laser-assisted machining of aluminum oxide ceramics with Taguchi method, Int. J. Mach. Tool Manufact. 47 (1) (2007) 141–147.

[19] Y. Liang, S.P. Dutta, Application trend in advanced ceramic technologies, Technovation 21 (1) (2001) 61–65.

[20] T.G. Bifano, T.A. Dow, R.O. Scattergood, Ductile-regime grinding: a new technology for machining brittle materials, J. Eng. Ind. 113 (2) (1991) 184–189.

[21] S. Malkin, C. Guo, Thermal analysis of grinding, CIRP Annals 56 (2) (2007) 760–782.

[22] M. Szkodo, et al., The influence of the depth of cut in single-pass grinding on the microstructure and properties of the C45 steel surface layer, Materials 13 (5) (2020) 1040.
[23] Z.J. Pei, A. Strasbaugh, Fine grinding of silicon wafers, Int. J. Mach. Tool Manufact. 41 (5) (2001) 659–672.
[24] C. Park, et al., The influence of abrasive size on high-pressure chemical mechanical polishing of sapphire wafer, Int. J. Precision Eng. Manuf.- Green Tech. 2 (2) (2015) 157–162.
[25] H. Singh, P.K. Jain, Lapping, in: V.K. Jain (Ed.), Nano-finishing Science and Technology: Basic and Advanced Finishing and Polishing Processes, CRC Press, 2016, pp. 79–92.
[26] T. Lee, et al., Self-dressing effect using a fixed abrasive platen for single-sided lapping of sapphire substrate, J. Mech. Sci. Technol. 31 (12) (2017) 5649–5655, https://doi.org/10.1007/s12206-017-1105-1.
[27] T. Yin, et al., Characteristic of SiC slurry in ultra precision lapping of sapphire substrates, Int. J. Precis. Eng. Manuf. 22 (6) (2021) 1021–1029, https://doi.org/10.1007/s12541-021-00521-1.
[28] Xiaohai Zhu, et al., Experimental study and modelling of the effect of mixed size abrasive grits on surface topology and removal rate in wafer lapping, Wear 305 (1–2) (2013) 14–22, https://doi.org/10.1016/j.wear.2013.05.007.
[29] Sumeet Bhagavat, et al., Effects of mixed abrasive grits in slurries on free abrasive machining (FAM) processes, Int. J. Mach. Tool Manufact. 50 (9) (2010) 843–847, https://doi.org/10.1016/j.ijmachtools.2010.04.006.
[30] Bo Xing, et al., Study on ultrasonic-assisted lapping performance and material removal behavior of diamond/SiC composites, Diam. Relat. Mater. 151 (2025) 111767, https://doi.org/10.1016/j.diamond.2024.111767.
[31] J. Chen, et al., Influence of agglomerated diamond abrasive wear on sapphire material removal behaviour, Diam. Relat. Mater. 108 (2020) 107965, https://doi.org/10.1016/j.diamond.2020.107965.
[32] J. Yun, et al., Effect of the properties of uniformly patterned micro-diamond pellets on sapphire grinding, J. Kor. Phys. Soc. 73 (7) (2018) 871–876, https://doi.org/10.3938/jkps.73.871.
[33] S. Gao, et al., Surface integrity and removal mechanism in grinding sapphire wafers with novel vitrified bond diamond plates, Mater. Manuf. Process. 32 (2) (2017) 121–126, https://doi.org/10.1080/10426914.2016.1140194.
[34] H. Kim, et al., Comparison between sapphire lapping processes using 2-body and 3-body modes as a function of diamond abrasive size, Wear 332–333 (2015) 794–799, https://doi.org/10.1016/j.wear.2015.02.029.
[35] A. Barylski, N. Piotrowski, Non-conventional approach in single-sided lapping process: kinematic analysis and parameters optimization, Int. J. Adv. Manuf. Technol. 100 (1–4) (2019) 589–598.
[36] N. Macerol, et al., A lapping-based test method to investigate wear behaviour of bonded-abrasive tools, CIRP Ann. - Manuf. Technol. 71 (1) (2022) 305–308, https://doi.org/10.1016/j.cirp.2022.04.049.
[37] S. Jianxiu, et al., Study on lapping paste of 6H–SiC single-crystal substrate in tribochemical mechanical lapping, J. Inst. Eng. India. Ser. 101 (2020) 141–148, https://doi.org/10.1007/s40034-020-00167-0.
[38] H.J. Pyun, et al., Fabrication of high performance copper-resin lapping plate for sapphire: a combined 2-body and 3-body diamond abrasive wear on sapphire, Tribol. Int. 120 (2018) 203–209.
[39] L. Guo, et al., An experimental study on the precision abrasive machining process of hard and brittle materials with ultraviolet-resin bond diamond abrasive tools, Materials 12 (1) (2019) 125, https://doi.org/10.3390/ma12010125.
[40] M. Deja, D. Zieliński, S.W. Agebo, Study on the wear characteristics of a 3D printed tool in flat lapping of Al2O3 ceramic materials, Wear 556 (2024) 205515.
[41] M. Deja, Simulation model for the shape error estimation during machining with flat lapping kinematics, in: ASME 2010 International Manufacturing Science and Engineering Conference, MSEC2010 - Erie, Pennsylvania, USA, 2010, pp. 1–9, https://doi.org/10.1115/MSEC2010-34262.
[42] A. Barylski, M. Deja, Wear of the tool in double-disc lapping of silicon wafers, ASME 2010 Int. Manu. Sci. Eng. Conf. 1 (2010) 301–307, https://doi.org/10.1115/MSEC2010-34323.